FZD-513

# Study of High Temperature and High Density Plasmoids in Axially Symmetrical Magnetic Fields

## Abschlussbericht

A. V. Anikeev, P. A. Bagryansky, V. V. Prikhodko,
E. I. Soldatkina. Yu. A. Tsidulko, E. Yu. Kolesnikov,
A. A. Lizunov, K. Noack, J. Konheiser, T. Berger

Februar 2009

Wissenschaftlich-Technische Berichte
FZD-513 2009 · ISSN 1437-322X

WISSENSCHAFTLICH-TECHNISCHE BERICHTE

Forschungszentrum
Dresden Rossendorf

Wissenschaftlich-Technische Berichte
**FZD-513**
Februar 2009 – Abschlussbericht

A. V. Anikeev, P. A. Bagryansky, V. V. Prikhodko
E. I. Soldatkina, Yu. A. Tsidulko, E. Yu. Kolesnikov,
A. A. Lizunov, K. Noack, J. Konheiser, T. Berger

# Study of High Temperature and High Density Plasmoids in Axially Symmetrical Magnetic Fields

Forschungszentrum
Dresden Rossendorf

**Institutional Partnership**

of

**Alexander von Humboldt Foundation**

Partners: Budker Institute of Nuclear Physics Novosibirsk,
Russian Academy of Sciences, Siberian Branch, Russia
and
Institute of Safety Research of Forschungszentrum Dresden-Rossendorf, Germany

# Final Report

on the joint research project

*Study of High Temperature and High Density Plasmoids in Axially Symmetrical Magnetic Fields*

Authors: A. V. Anikeev, P. A. Bagryansky, V. V. Prikhodko,
E. I. Soldatkina, Yu. A. Tsidulko, E. Yu. Kolesnikov,
A. A. Lizunov
*Budker Institute of Nuclear Physics Novosibirsk*

K. Noack, J. Konheiser, T. Berger
*Forschungszentrum Dresden-Rossendorf*

Publication Date: February 2009

**Content**

## 1. Introduction

The experimental and theoretical activities at the gas dynamic trap (GDT) experimental facility of the Budker Institute of Nuclear Physics Novosibirsk (BINP) aim at the investigation of fundamental scientific problems which are of actual interest for axial-symmetric plasma machines such as the quality of the magnetic plasma confinement, plasma stability and plasma transport phenomena. At the same time, the research is application oriented: The investigation results fill up the data bank which will serve as the basis for the design of an intense fusion neutron source. The Budker Institute has made the proposal of a GDT based 14-MeV neutron source as irradiation facility for fusion material research [1, 2]. A complete experimental/ analytical database on plasma confinement, stability and transport phenomena is mandatory for the final design of the neutron source. In the context of mirror approach to fusion reviewed e. g. in Ref. [3], this neutronic application of a GDT type machine can be considered as short-term application of a mirror fusion device. Compared with other fusion neutron sources, the GDT based one should have several principal advantages [2].

The GDT experimental facility of the Budker Institute is a long axial-symmetric magnetic mirror with a high mirror ratio $R$ which can be varied in the range 12.5 – 100. The magnetic field confines a two-component plasma. One component is a collisional "background" plasma (alternatively also called “target” plasma) with ion and electron temperatures presently up to 100 eV and a density up to $5\times10^{13}$ cm$^{-3}$. For this component, the ion mean free path of scattering into the loss cone is much less than the mirror-to-mirror distance what results in the gas dynamic regime of confinement. The second component is the population of high-energy protons or deuterons, called fast ions which have kinetic energies in the range of 2-25 keV and concentrate up to a particle density of $4\times10^{13}$ cm$^{-3}$. It is produced by neutral beam injection (NBI) shooting hydrogen or deuterium atoms into the centre of the central cell under an angle of 45° to the mirror axis. The fast ions are confined in the mirror regime having their turning points at the mirror ratio of 2. To provide MHD stability of the entire plasma, axial-symmetric minimum-B cells are attached to both ends of the device. The GDT facility is described in more detail e. g. in Refs. [4, 5].

At present, the GDT facility is being upgraded. The first stage of the upgrade is the installation of the experiment SHIP (**S**ynthesized **H**ot **I**on **P**lasmoid) within the GDT followed by experiments with this new coupled device. The idea of the SHIP experiment has been presented in Ref. [6]. The experiments should aim at investigating plasmas as they are expected to appear in the regions of high neutron production in a GDT based fusion neutron source. The plasma states in these regions are characterized by a high fast ion density of about $2\times10^{14}$ cm$^{-3}$ resulting in a high maximal value of plasma-$\beta$ in the range between 0.4 – 0.7 and in a high degree of anisotropy of the fast ion motion which is strongly peaked in the direction perpendicular to the magnetic field. Because of these particularities, questions arise regarding stability and equilibrium of such plasmas. They cannot be answered with sufficient confidence with theoretical and computational research alone but absolutely need appropriate experiments. Therefore, SHIP was a necessary step in the upgrade of the GDT facility.

Within the framework of an Institutional Partnership of the Alexander von Humboldt (AvH) Foundation, the BINP and Forschungszentrum Dresden-Rossendorf (FZD)

worked together in the present joint project devoted to the research at the coupled GDT-SHIP facility with the focus on the study of plasma phenomena within the SHIP mirror section. The project began at July 1st, 2005 and ended on August 30th, 2008. It included work packages of significant theoretical, computational and analyzing investigations. The immense volume of constructive and experimental works did not appertain to the project and was carried out by the GDT team under the leadership of Dr. P. A. Bagryansky.

The structure of this final report corresponds roughly that of the project application. However, the focus is on the presentation of results achieved whereas the work that was done is described briefly only. Chapter 2 illustrates the GDT-SHIP facility and describes the topics of the SHIP plasma research. Chapter 3 explains the main extensions and modifications of the **I**ntegrated **T**ransport **C**ode **S**ystem (ITCS) [7], which were necessary for appropriate calculations of the fast ion and neutral gas particle fields in SHIP, describes briefly the scheme of computations and presents significant results of pre-calculations from which conclusions were drawn regarding the experimental program of SHIP. In chapter 4, theoretical and computational investigations of self-organizing processes in two-component plasmas of the GDT-SHIP device are explained and the results hitherto achieved are presented. In chapter 5, significant results of several experiments with moderate and with enhanced plasma parameters are presented and compared with computational results obtained with the ITCS. Preparing neutron measurements which are planned for neutron producing experiments with deuterium injection, Monte Carlo neutron transport calculations with the MCNP code were also carried out. The results are presented. Finally, from the results obtained within the joint research project important conclusions are drawn in chapter 6.

## 2. Concept of the GDT-SHIP experiment

### 2.1. Description of the experimental set-up

Figure 1 shows the schematic layout of the GDT-SHIP facility.

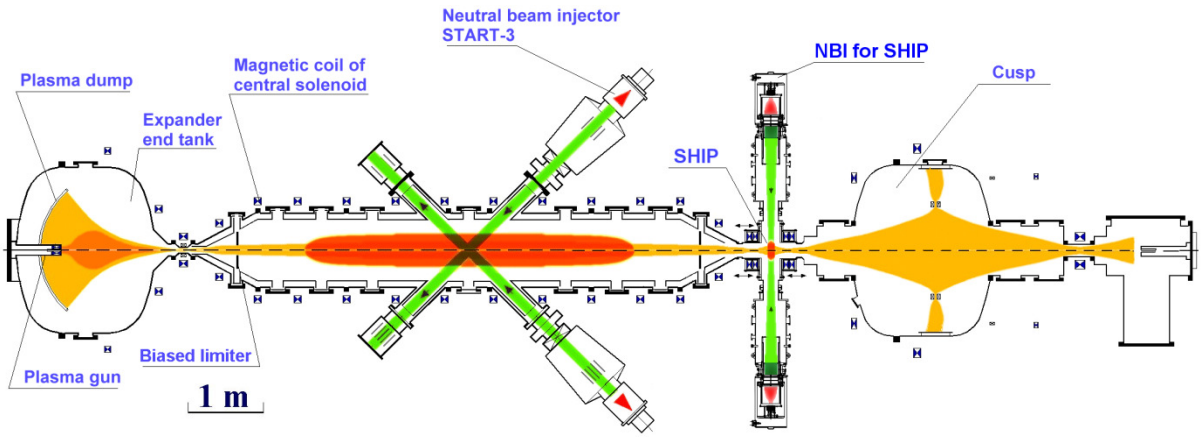


Fig. 1: Schematic layout of the GDT-SHIP facility.

The small mirror cell where “hot ion plasmoids” are to be synthesized has been installed just behind the mirror coil of the GDT central cell. The magnetic field is

illustrated in the diagrams of Fig. 2. In the centre of SHIP, the field strength can reach 2.5 Tesla. Then the mirror ratio is about 2. The magnetic field strength around the mid-plane can be varied by extending/shortening the distance between both mirror coils.

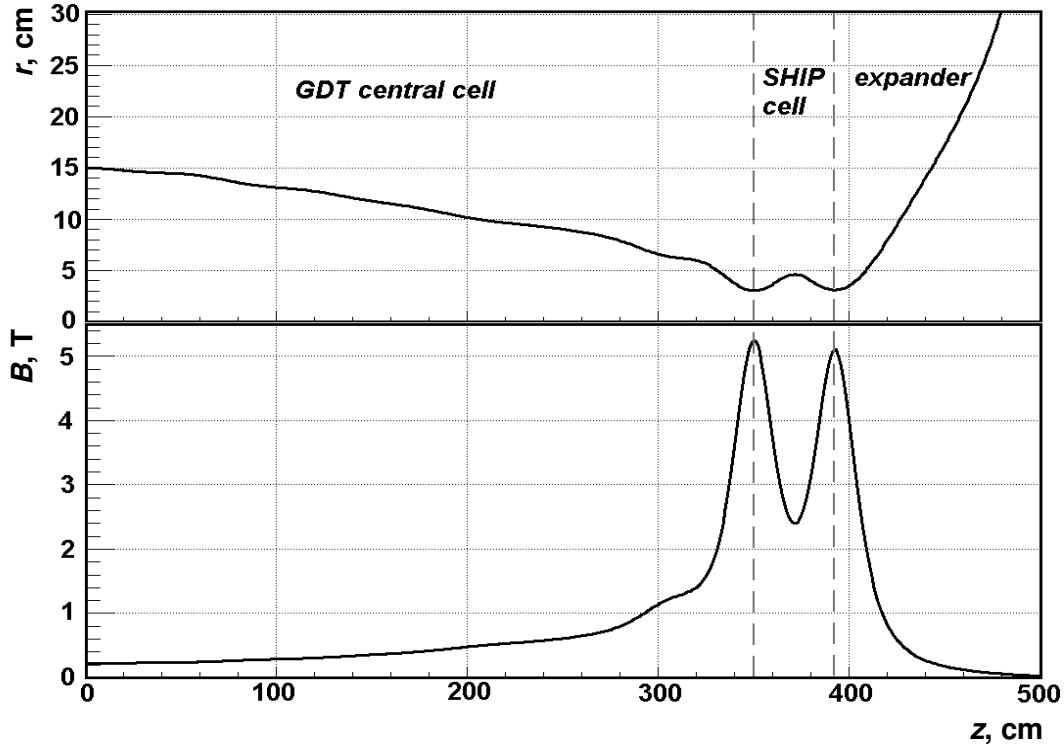


Fig. 2: A magnetic field line (top) and the on-axis magnetic field strength of the GDT-SHIP facility (bottom).

The SHIP cell is filled with background plasma streaming in from the GDT central cell. This plasma component is maxwellized. At present, typical values of its density and electron temperature are $10^{13}$ cm$^{-3}$ and 100 eV, respectively. It is pre-heated up by the standard NBI system of the GDT consisting of six injectors. Two newly developed neutral beam injectors should perpendicularly inject into SHIP focused beams of hydrogen or deuterium atoms with energy up to 25 keV as pulse with duration up to 4 milliseconds. Ionization of the beams by the target plasma generates the highly anisotropic fast ion component. The density of the resulting hot ion plasmoid is expected to be considerably higher than that of the target plasma ions.

The SHIP device is equipped with several diagnostic techniques which are already successfully used in GDT experiments [4] or have been especially designed for measurements at SHIP. Diamagnetic loop, $CO_2$–interferometer and MSE (motional Stark effect) diagnostics allow one to measure the total plasma energy, the line-integrated density of electrons and the $\beta$-parameter which is defined as ratio of plasma pressure to magnetic field pressure, respectively. A charge-exchange (CX) analyser has been designed for observation of the fast ions spatial distribution. A radio-frequency (RF) 8-mm interferometer and an ion current detector are placed inside the expander tank beyond the mirror to measure linear density and ion current of the plasma leaving the central cell and the SHIP cell along the field lines and flying to the end wall. Likewise, neutron detectors will be installed outside the SHIP

container for observation of fusion reactions between fast ions in case of deuterium injection.

## 2.2. Objectives of SHIP research

Just after the start of the project the spectrum of possible investigations which are of interest both for mirror plasma physics and for the neutron source project were intensively discussed. A part of the proposed topics were already aimed at in Ref. [6] where the SHIP experiment had been proposed. The discussion based on the results of rough analytical estimates of the fast ion field that was expected to be synthesized by perpendicular neutral beam injection. It was assumed that a fast ion density of more than $10^{14}$ $cm^{-3}$ in a volume of nearly 500 $cm^3$ could be achieved with two new neutral beam injectors. The mean energy of these ions should be around 15 keV provided their injection energy is near to 25 keV. Together with the possibility to vary the magnetic field strength, such parameter values should make possible to carry out experiments with plasma-$\beta$ within in the broad range between 0.01 – 0.7. $\beta$ is a fundamental plasma physical parameter which is defined as ratio of perpendicular plasma pressure to magnetic field ($B$) pressure

$$\beta = \frac{8\pi \cdot P_f}{B^2}. \qquad (1)$$

In case of SHIP the plasma pressure is definitely determined by the fast ion pressure $P_f$ alone. In this way, the SHIP experiment offers the unique chance to study plasma effects connected with such high fast ion densities at high $\beta$-values which both are in ranges such as required for the neutron source project. In addition, several features of the plasma, like the composition of two energetically very different ion components from which the high-energy part represents the majority, strong non-isotropic angular distribution of the high-energy ions and non-linear effects as non-paraxial effective magnetic field together with high $\beta$ offer a broad field for new plasma-physical investigations. The following questions are of fundamental interest for two-component GDT type plasmas in axial-symmetric magnetic confinements and have direct effect on the neutron source project:

- What are the attainable maximum parameters of stable background plasma and of fast ions?
- The highly anisotropic fast ion velocity distribution results in distortion of the total magnetic field which becomes non-paraxial even if the external magnetic field is paraxial. How does the non-paraxiality impact on plasma equilibrium?
- Do essential self-organizing effects appear within the plasma under such conditions and, especially, do they result in a pinching of the fast ion distribution in space what would yield higher neutron source intensities?
- What are the effects of non-paraxiality on the MHD stability of the SHIP plasma and what is the contribution to the overall MHD stability of the whole GDT facility?
- The gyrating fast ions can interact with electro-magnetic plasma waves of various types. Such micro-fluctuations can lead to a rapid loss of their energy or even to an increase of their outflow through the mirror coils. Is there a $\beta$-

threshold for these micro-fluctuations? If so, then its dependencies on the anisotropy of the fast ion velocity distribution and on the non-praxiality of the magnetic field should be investigated.

The answers to these and other questions are the objectives of the experimental and theoretical research at the GDT-SHIP facility.

The joint AvH research project involved theoretical and computational work of the starting phase of the entire SHIP research program. Terminating a long-time collaboration between both partners, the project was also used to finally hand over to BINP the fast ion and neutral gas codes of the ITCS which have been developed by FZD.

## 3. Adaptation and upgrade of ITCS and MCNP and calculations of GDT-SHIP experiments

### 3.1. Extensions and modifications of transport codes

The experimental GDT-SHIP research program is accompanied by computations with numerical codes of the Integrated Transport Code System. This code system has been developed in recent years in collaboration between the Institute of Safety Research of the Research Centre Dresden-Rossendorf and the Budker Institute [7]. Its modules allow to simulating the behavior of target plasma and fast ion field in the frame of classical plasma physics under consideration of their interactions among each other and with neutral gas and magnetic field. The experiments with the upgraded GDT-SHIP facility establish new physical conditions which demanded essential extensions, modifications and careful adaptation of the codes to these conditions. In this section the important extensions/modifications of ITCS codes will be shortly described and the main results of a series of pre-calculations will be presented.

Apart from ITCS codes, the neutron transport code MCNP [8] was used for computing the neutron field which is produced in SHIP experiments with deuterium neutral beam injection. An inspection of the possibilities offered by this code made clear that no special modifications of the code are necessary for the planned computations. The only measure which has to be taken is the approximate fitting of the neutron source distribution in space by analytical expressions offered by MCNP.
The neutron source must be calculated from the fast ion density distribution supplied by MCFIT (see subsection 3.1.1.) with help of the auxiliary ITCS code MAXIM.

#### 3.1.1. Fast ion transport code MCFIT

The behaviour of the fast ion field in the gas dynamic trap is the crucial topic of the GDT based neutron source project. The fusion reactions occurring in collisions between fast deuterons and tritons release the desired neutrons. During their life-time the fast ions interact with a given magnetic field, target plasma and with neutral gas. The **M**onte **C**arlo **F**ast **I**on **T**ransport code MCFIT simulates the transport of neutral beam produced high-energy ions and allows the computation of a broad spectrum of quantities which are related with the fast ion field [9, 10]. The code is based on the fundamental assumption of a linear and classical fast ion transport but presupposes only a minimum of further approximations. The simulation models used

by MCFIT correspond to the following transport equations written for the particle densities $n_f = n_f(\vec{r}, v, \vec{\Omega}, t)$ of fast ions of type $f=H^+, D^+, T^+$:

$$\frac{\partial}{\partial t} n_f + \left[ v\vec{\Omega} \frac{\partial}{\partial \vec{r}} + \frac{q_f}{m_f} \left( v\vec{\Omega} \times \vec{B}(r,z,t) \right) \frac{\partial}{\partial \vec{v}} \right] n_f = \frac{1}{v^2} \frac{\partial}{\partial v} \frac{v^3}{\tau_{v,f}} n_f + \frac{1}{4\tau_{d,f}} \nabla^2_{\vec{\Omega}} n_f - g(r,z,t) \langle \sigma v \rangle_{cx,f} n_f + S_f(\vec{r}, v, \vec{\Omega}, t) \quad (2)$$

In Eq. (2) mean:

- $\vec{r}$ - Space point in cartesian co-ordinates: *x, y, z* or in axial-symmetric magnetic field co-ordinates *r(z), φ, z*. The radial co-ordinate *r* varies with the axial co-ordinate *z* according to $r(z) = r_0 / \sqrt{B_0(z)}$ where $B_0$ is the on-axis magnetic field strength.
- $\vec{v}$ - Velocity vector with $v = |\vec{v}|$ as the flight speed of a particle.
- $\vec{\Omega}$ - Unit vector of the flight direction. The velocity vector is $\vec{v} = v\vec{\Omega}$.
- $t$ - Time.
- $n_f(\vec{r}, v, \vec{\Omega}, t)$ - Particle density in phase space of fast ions of type *f*.
- $q_f$ - Electrical charge of a fast ion of type *f*.
- $m_f$ - Mass of a fast ion of type *f*.
- $\vec{B}(r,z,t)^*$ - Vector of the axial-symmetrical magnetic field. The magnetic field strength is $B = |\vec{B}|$. The space and time dependencies of its *r*- and *z*-components must be input into MCFIT.
- $\tau_{v,f}{}^*$ - Slowing down (drag) time of a fast ion of type *f*. It is determined by electron density $n_e$ and electron temperature $T_e$. With regard to the neutron source, this quantity should be as large as possible.
- $\tau_{d,f}{}^*$ - Deflection time of a fast ion of type *f*. It is determined by the densities $n_f$ of fast ions and $n_w$ of so-called “warm ions” of the target plasma. Regarding the neutron source, this quantity should be as large as possible.
- $\nabla^2_{\vec{\Omega}}$ - Angular part of the Laplace operator.
- $g(r,z,t)^*$ - Axial-symmetrical particle density of the neutral gas. The quantity *g* stands symbolically for neutral gas. Actually, it consists of three components. Their space and time dependencies must be input into MCFIT. Since the interaction with the neutral gas results in a loss of fast ions, the gas density should be as small as possible. See also subsection 3.1.2.
- $\langle \sigma v \rangle_{cx,f}$ - Effective microscopic reaction rate of the charge-exchange process of a fast ion of type *f* with the neutral gas.
- $S_f(\vec{r}, v, \vec{\Omega}, t)^*$ - Distribution of the fast ion birth rate. This distribution is stochastically generated by MCFIT. To this end, data giving information on neutral beam injectors, electron density $n_e$ and warm and fast ion densities $n_w$ and $n_f$, respectively, must be input into MCFIT. To get a maximal neutron emission intensity in the neutron source, this ionization rate should be maximal.

Eq. (2) is a particle balance equation in infinitesimal phase space elements relating the fast ion density changes in time to several transfer processes occurring in phase space. The second term on the left-hand side represents the collision-less Larmor-movement of an ion in an axial-symmetrical magnetic field which can be time dependent. The first term on the right-hand side describes the continuous slowing down of the high-energy ions by Coulomb interactions with other charged particles. The drag by the electrons is the superior part of this process. The second term on the right-hand side describes the diffusion-like deflection of the flight direction of an ion that flies through plasma. This process is dominated by Coulomb collisions with ions. The third term represents the particle loss by charge-exchange with neutral particles which are on the way of the moving fast ion. In this case the ion becomes a "fast neutral" and the neutral atom or molecule will be ionized and starts its Larmor-movement as ion. The source term $S_f$ represents the distribution in phase space of the fast ion birth rate. The neutral particles (in case of GDT-SHIP – hydrogen or deuterium atoms and in case of the GDT based neutron source – a mixture of deuterium and tritium atoms) which are injected by the NBI´s into the target plasma are partly ionized by various interaction processes and form the source of fast ions. Details on the background of classical plasma theory can be found in plasma physics textbooks, for instance in Ref. [11]. More details on the simulation procedures of various processes realized in MCFIT are given in Refs. [9, 10].

The explanations given before make clear that the fast ion transport is a linear one provided that, firstly, magnetic field, target plasma and neutral gas do not depend on the fast ion field and, secondly, that no relevant contributions to angular scattering and ionization of the NBI´s are produced by the fast ions themselves. This frame of linear classical behaviour of the fast ions proofed to be valid in GDT experiments carried out before the upgrading of the facility. Measurement and calculation results agreed very well what was a consequence of the low fast ion density in these experiments [4]. In GDT-SHIP experiments the situation will be substantially different from that in GDT experiments. Rough estimates showed that the fast ion density in SHIP must be expected to be remarkably higher than that of the target plasma ions and will reach such values causing several non-linear phenomena. Subsequently, the phenomena through which non-linearities enter into the fast ion transport will be discussed. The corresponding quantities or functions appearing in Eq. (2) are labelled with an asterisk in the list above.

a. Magnetic field $\vec{B}(r,z,t)$:
   The movement of the fast ions in the magnetic valley of SHIP is a superposition of the gyration around magnetic field lines and an azimuthal drift mainly caused by the $\vec{B}\times\nabla B$ (gradient) force. As result, the ions form a disk in which a net azimuthal current appears growing radial outward. This net current generates its own magnetic field. Therefore, the effective magnetic field acting on a fast ion is the sum of external field $\vec{B}_{vac}$ produced by the coils without plasma and of the internal field $\vec{B}_{int}(n_f)$ generated by the fast ions themselves

$$\vec{B} = \vec{B}_{vac} + \vec{B}_{int}(n_f)\,. \tag{3}$$

The internal field is oriented against the external field, so that one hast to expect a reduction of the total magnetic field strength around the centre of the fast ion disk. This distortion of the magnetic field could cause a noticeable redistribution of fast ions in space. This effect is the so-called "high-$\beta$ effect". It grows up if the fast ion current increases by higher density and/or kinetic energy and, to certain extend, if the magnetic field strength is reduced.

To have an option for considering this non-linear effect in computations, in MCFIT the calculation of the net fast ion current over a (*r,z*)-bin structure was incorporated. This current profile is output and the produced magnetic field $\vec{B}_{int}$ is externally calculated by means of the auxiliary ITCS code FITMAG according to the law of Biot-Savart. For a next MCFIT calculation the total field $\vec{B}$ according to Eq. (3) can be input instead of $\vec{B}_{vac}$.

b. Target plasma:
In fast ion simulations of former GDT experiments it was sufficient to describe the target plasma as a neutral mixture of electrons and ions characterized by the same particle density and temperature fields. However, another situation appears in SHIP experiments which should be simply explained. The background plasma enters the SHIP mirror from the GDT central cell with time dependent radial profiles: $n_0$ – ion and electron densities, $T_e$ and $T_i$ – electron and ion temperatures, respectively, which are both near to each other, typically around 100 eV. Because the target plasma ions have essentially lower energy than the fast ions, they are also called "warm ions". The particle densities and temperatures disperse along the magnetic field lines over the plasma volume in SHIP. The neutral beams are partly ionized by various collision reactions with electrons and warm ions. Because of the intense production of fast ions an ambipolar electrostatic potential is generated which expels other ions to enter this volume and attracts electrons. In consequence, the density of warm ions is reduced $n_w<n_0$ and the electron density is increased $n_e>n_0$. These changes of the particle densities have an impact on the ionization of the neutral beams and on the fast ion transport. At present, there is no numerical code available which is capable to adequately compute the target plasma under such conditions. Instead of this, an approximate analytical model was developed and was applied in all fast ion computations for SHIP so far. Next, this model should be briefly outlined.

In an electrostatic potential $\varphi$, electrons and warm ions are distributed in accordance with Boltzmann´s law

$$n_e = n_0 \cdot \exp(e\varphi / kT_e) \tag{4}$$

$$n_w = n_0 \cdot \exp(-e\varphi / kT_w)\,. \tag{5}$$

In Eq. (5), $T_w$ is the temperature of the warm ions. All densities and temperatures are functions of radius *r*, axial co-ordinate *z* and of time *t*. $n_0(r,t)$ is the radial profile of the target plasma streaming in from the central cell and is assumed to be independent on the processes occurring in SHIP. Assuming

that approximately $T_w = T_e$ and considering the neutrality condition for the whole plasma

$$n_e = n_w + n_f \ , \tag{6}$$

one gets the relationship

$$n_w = \left( \sqrt{n_f^2 + 4n_0^2} - n_f \right) / 2 . \tag{7}$$

Eqs. (6, 7) give the dependencies of the target plasma constituents $n_e$ and $n_w$ on the fast ion density in SHIP for a given inflow of an independent target plasma $n_0$.

Analogously as with the high-$\beta$ effect described in a., the effect of the ambipolar potential can be taken into consideration only iteratively by subsequent MCFIT computations. For instance, assuming $n_f^0 = 0$ and $n_e^0 = n_w^0$, from the first MCFIT computation one gets an approximate fast ion density $n_f^1$, which supplies from Eqs. (6, 7) approximate densities $n_e^1$ and $n_w^1$ for the second MCFIT computation and so on.

The different density and temperature fields of warm ions and electrons were introduced in MCFIT and taken into consideration in all routines simulating the energy slow down ($\tau_{v,f}$), the angular scattering ($\tau_{d,f}$) and the neutralization processes ($S_f$) of the neutral beams. Comparisons between measurement and calculation results show that relationship (6, 7) is an acceptable approximation for plasmas which occurred in SHIP so far.

c. Interaction with the field of fast ions:
A fast ion test particle, the history of which is simulated by MCFIT, interacts also with the fast ion field directly. In general, the quantities $\tau_{v,f}$, $\tau_{d,f}$ and $S_f$ include terms from the fast ion field. Therefore, the previous code version had to be modified correspondingly. The fast ion densities so far achieved in SHIP experiments show the following situation:
   - The fast ion field practically does not contribute to the slowing down. This process remains determined by the electron drag alone.
   - Compared with the warm ions, the contribution of the fast ions to angular scattering becomes important and must not be neglected.
   - Now, the module of MCFIT simulating the ionization processes of the injected neutral beams includes the ion impact with fast ions too. So, the new code considers the ionizations by: charge exchange and impact with warm ions ($n_w$), electron impact ($n_e$) and impact with fast ions ($n_f$). The latter process gave typically about 15 % of the total ionization rate in last SHIP experiments.

MCFIT starts the simulation of fast ion “test” particles with the injection of corresponding neutrals by a number of neutral beam injectors. One sub-task of the GDT upgrading was the design and construction of a new injector type and installing them at SHIP and at GDT. In addition to higher beam parameters of current and energy, the new injectors are equipped with an ion-optic which is capable to focus the neutral beam in different degree with respect to both axes of the beam cross-

section. This new option of neutral beam injection was incorporated in the injection routines and the concrete values of free parameters were determined by special measurements.

### 3.1.2. Neutral gas transport code NEUFIT

For the calculation of the fast ion density distribution in a gas dynamic trap it is necessary to consider their interaction with the neutral gas (denoted with *g* in Eq. (2)) which is inside the vacuum chamber and is fed by various gas sources. The rate of mutual reactions between gas particles is negligibly small. The deterministic computer code NEUSI makes possible to calculate the distributions of neutral gas components in long axial-symmetrical devices like the GDT [12]. It bases on the linear integral transport method which is commonly used for solving neutron transport problems. The code makes use of the approximate assumption that the radius of the chamber is small in comparison with its length. This approximation is not justified for the SHIP device. Therefore, the new gas transport code NEUFIT, which avoids this approximation, has been developed on the base of NEUSI. In addition, an improved simulation of the neutral-wall interaction was incorporated. The basic physical models governing the transport of neutrals are described in Refs. [9, 12, 13].

The high-energy hydrogen atoms injected as neutral beams interact with ions and electrons of the target plasma. Charge-exchange reactions with warm ions produce fast ions and “slow” hydrogen atoms with energies less than 500 eV. These “slow atoms” represent the dominant primary gas source. During their life histories, the fast ions interact with the neutral gas components. By charge-exchange with slow neutral atoms, they become “fast atoms” having energies above 500 eV up to the injection energy. Moreover, the target plasma interacts with neutral gas components and produces fast and slow neutrals too. A certain part of the neutral atoms, which were born inside the plasma, flies to the wall of the vacuum chamber without being ionized. A part of them will be reflected with reduced energy. NEUFIT approximately assumes that all reflected atoms are “slow” ones. The other part accumulates on the wall surface as hydrogen molecules which return into the chamber volume with low energies corresponding to the wall temperature. The recycling coefficient of the wall used in these simulations was put equal to one. This value has been confirmed by a study of the fast titanium coating of the GDT first wall [13].

Altogether, there are three components of neutral hydrogen gas in the facility: slow atoms, fast atoms and hydrogen molecules. NEUFIT calculates their density distributions over a (*r,z*)-grid inside the SHIP volume during an experimental shot for given time courses of fast and warm ion distributions $n_f$ and $n_w$, respectively. The energy dependencies of the various interactions of the neutrals are considered in the so-called energy group approximation. Regarding the space dependency, the code assumes that the problem is an azimuthally symmetric one. The primary gas source of slow atoms that is produced by the neutral beams does not fulfill this assumption. But, the fast ions show a strong azimuthal drift which reduces the effect of this approximation.

The fact that in SHIP experiments the neutral gas practically fills out the whole living space of the fast ions results in a relatively strong loss of them. This demands the consideration of realistic gas distributions when simulating the fast ion transport.

Likewise, the fact could prevent to reach very high fast ion densities which were expected when SHIP had been designed.

### 3.2. Iterative application of ITCS codes for SHIP plasma calculations

The explanations given in the preceding two subsections made clear that both MCFIT and NEUFIT are codes which simulate a linear fast ion transport or solve a linear transport equation for the neutral gas, respectively. Therefore, the non-linear effects discussed must be considered by iteration of calculations. The basis of such an iteration scheme with one or several codes is the exchange of appropriate data. For this purpose the codes output and read in the following quantities which they calculated or require, respectively. The iteration scheme of the ITCS codes was perfected by the work within the present project.

- MCFIT
  - Output:
    - $n_f(r,z,t)$ - The fast ion density for corrections of $n_w$, $n_e$, $\tau_{v,f}$, $\tau_{d,f,}$ $S_f$ in MCFIT and for taking into account the mutual reaction with the fast ions in the gas transport calculation with NEUFIT.
    - $f(\theta;r,E,t)$ - The pitch-angle ($\theta$) distributions of the fast ions in the SHIP mid-plane for an user-defined grid in radius, energy and time. These functions are used by MCFIT in the simulation of the NBI ionization $S_f$ and for computing the neutron production rate by DD- or DT-fusion reactions.
    - $f(E;r,t)$ - The energy spectra of the fast ions for an user-defined $(r,t)$-grid. These functions are used by the NEUFIT code for modeling the interaction between neutral gas components and fast ions.
    - $j(r,z,t)$ - The net azimuthal fast ion current density over an user-defined grid in $r$, $z$ and $t$. With this current profile the internal magnetic field $\vec{B}_{int}$ can be calculated by means of the auxiliary code FITMAG, see subsection 3.1.1.
    - $S_{sla}$ - A data file which collected the co-ordinates and kinetic parameters of slow atoms which are produced in the simulation of the neutral beam ionization by charge-exchange reactions with warm ions, see subsection 3.1.2. These data represent the primary gas source for the NEUFIT code. The data file can be generated by a special “short” MCFIT run which simulates only the injection of the neutral beams and their ionization without the time-consuming simulation of the fast ion transport.
  - Input:
    - $n_f(r,z,t)$ from a preceding MCFIT calculation.
    - $f(\theta;r,E,t)$ from a preceding MCFIT calculation.
    - $g(r,z,t)$ - The density distributions of the three neutral gas components.

    For explanations of the functions see above.

- NEUFIT
  - Output:
    - $g(r,z,t)$.
  - Input:
    - $n_f(r,z,t)$, $f(E;r,t)$ and $S_{sla}$.

From the iterative computations of SHIP experiments which were done so far the following significant experience could be gained:

a. The consideration of the effect of the ambipolar potential is absolutely mandatory. The application of the approximate model defined by Eqs. (6, 7) within subsequent MCFIT calculations gives the decisive contribution to the good agreement between calculation and measurement results. The convergence of the iteration scheme turned out to be relatively fast: Not more than 3 – 4 MCFIT calculations were necessary to get into the fluctuation range of about 5 % which is considered to be sufficient for this type of complex calculations.
b. Test calculations showed that the iteration which is necessary for taking into account the high-$\beta$ effect could be made in parallel with the iteration for the ambipolar potential (see under a.).
c. Test calculations showed that the iteration between fast ion field and neutral gas could be considerably simplified without noticeably losing in accuracy. The field analyses of the three neutral gas components revealed that their distribution in space differs only weakly for different plasma conditions in SHIP. However, their amplitudes clearly depend on the intensity of the primary gas source of slow atoms which is proportional to $n_w$. This fact led to the following standard iteration scheme: The three gas components are computed by NEUFIT only once at the beginning of the iteration cycle. Between two successive MCFIT simulations (see under a.) when the target plasma composition ($n_w$ and $n_e$) is updated, by means of a "short" MCFIT run information on the intensity of the new primary gas source is derived. Correspondingly, the amplitudes of the three gas fields are corrected and then used as the new neutral gas in the next MCFIT simulation. In this way, no further gas field computations with NEUFIT are necessary.

### 3.3. Illustrative examples of calculation results

To illustrate the basic physical situation in SHIP experiments, some diagrams which represent important ITCS calculation results will be shown and commented in the following. Figures 3 and 4 show the steady state radial (in the mid-plane) and axial (on the axis) density distributions of the plasma components, respectively, as they were computed for a series of experiments with a NBI power of 1 MW. The calculation model corresponds to the proposed experimental regime *v.2* specified in Table 1 in subsection 3.4. The density distributions shown are computed for the time moment when the fast ion density $n_f$ is in its maximum.

The results of the codes MCFIT and NEUFIT are actually histograms over an user-defined interval grid of the variables. The continuous curves in the figures were obtained by smoothing the histograms by means of standard software.

It turned out that the fast ion density reached its steady state rather quickly in about 1 millisecond. The maximum of the fast ion density distribution remained in the range of the statistical error of a few per cent after four iteration steps. Its value is predicted by the computations with about $8\times10^{13}$ cm$^{-3}$. The curves illustrate the small extension of the SHIP plasma both in radial and in axial direction which are about 5 cm each. The first fact is caused by the tight target plasma column and the second by the focusing of the neutral beams and by the small length of the SHIP mirror. The figures

show the strong effect of the splitting up of warm ion density and of electron density which is caused by the ambipolar potential. One can see that the fast ion density is higher than that of the warm ions in the greater part of the plasma volume. It is about 600 $cm^3$. Moreover, in Fig. 3 one can see a small radial depression of the fast ion density near to the axis which is caused by the high-$\beta$ effect. In more detail it will be demonstrated below.

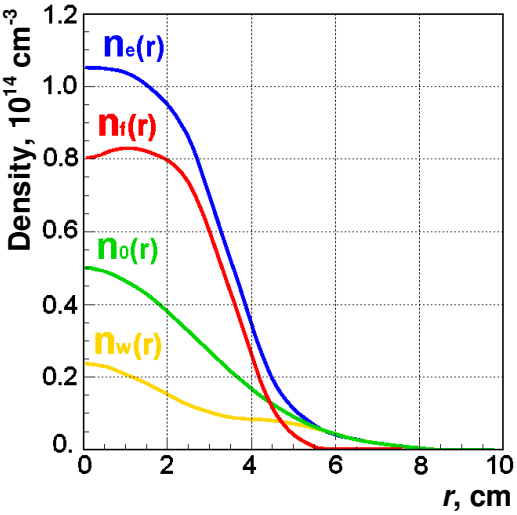


Fig. 3: Radial distributions of particle densities.

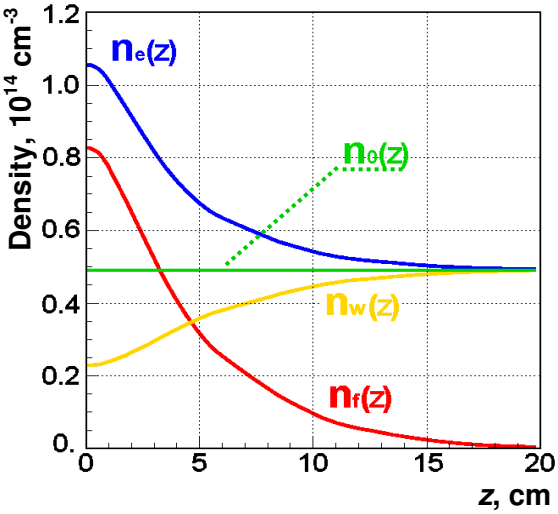


Fig. 4: Axial distributions of particle densities.

Figure 5 shows the radial distributions of the three neutral gas components in the mid-plane of SHIP. They were computed with NEUFIT for the proposed experimental regime *v.2* defined in Table 1. The SHIP chamber has an inner radius of 34.6 cm. Because of the small radial extension of the fast ion field, only the radial range up to 10 cm is of importance. A noteworthy effect is that the hydrogen molecules cannot enter the inner plasma volume occupied by the fast ions. Obviously, they are ionized by the edge of the target plasma. Moreover, it is remarkable that in the range of the fast ions the density of the slow atoms remains essentially higher than that of the fast atoms despite of the strong lowering of the warm ion density by the ambipolar potential.

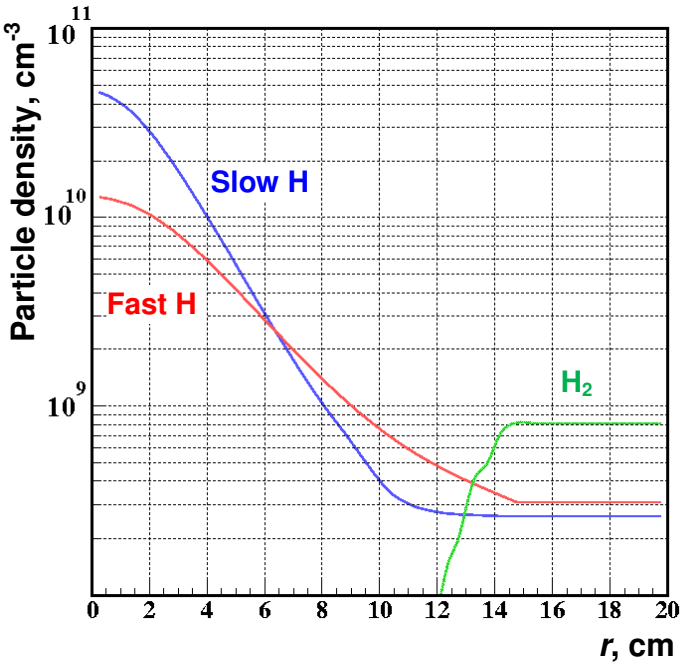


Fig. 5: Radial distributions of the neutral gas components.

As next example, which should be illustrated, calculation results of the high-$\beta$ effect are presented. To this end, the results obtained for the proposed experimental regime *v.5* such as defined in Table 1 is selected. This experimental regime is especially planned for investigations of the high-$\beta$ effect. In order to reach $\beta$-values in the range 0.4 – 0.7 the SHIP mirror will be axially somewhat elongated so that the magnetic field in the mid-plane will be reduced from 2.3 to 0.7 Tesla.

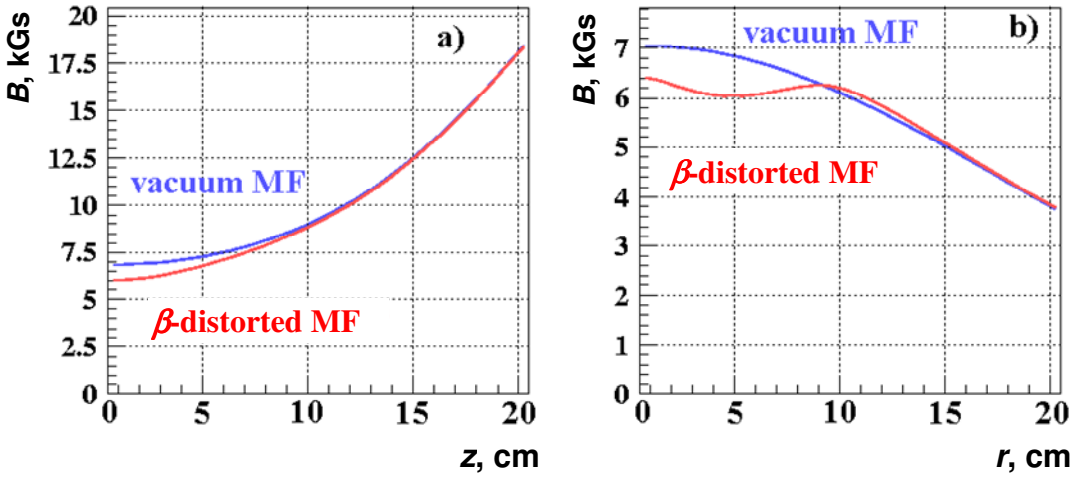


Fig. 6: The $\beta$-distortion of the magnetic field. a) On-axis profiles. b) Radial profiles.

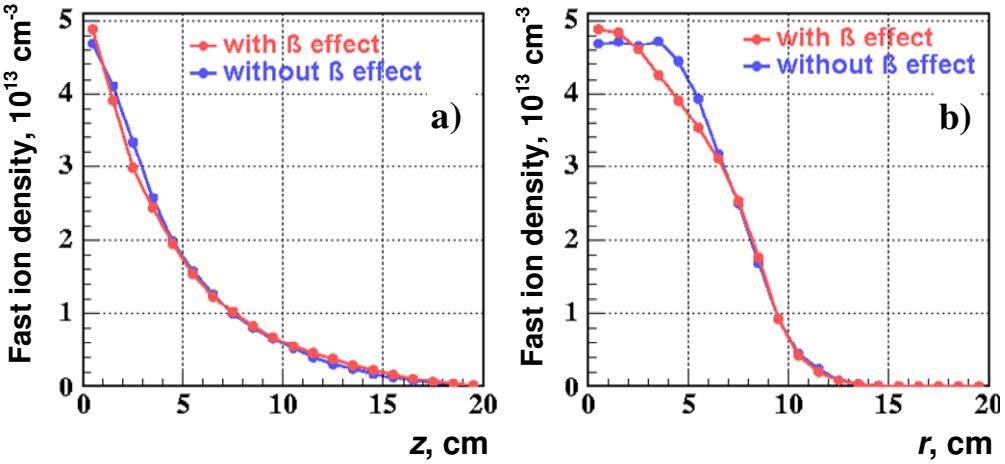


Fig. 7: High-$\beta$ effect on fast ion density profiles. a) On-axis profiles. b) Radial profiles.

Figures 6 a) and b) show the distortions of the magnetic field by the high $\beta$-value which was computed for $\beta$=0.62 (see Table 1). The blue curves are the magnetic field strength $B_{vac}$ in the vacuum case, i. e. without plasma, and the red curves are the strength of the total field according to Eq. (3). Analogously, Figs. 7 a) and b) show the relocation of the fast ion field which occurs in consequence of the magnetic field distortion. By means of the ITCS codes, the distortion was computed for 15 % only. Hence, the fast ion relocation is small. Only the radial profile shows a noticeable

squeezing of the density peak near to the axis. In contrast to this result, an estimate of the effect made with the approximate assumption of a paraxial magnetic field gives a distortion of about 30 %, provided the computed $\beta$-value is correct. However, the assumption of a paraxial field seems to be not justified in case of SHIP. Unfortunately, up to now the series of experiments under high-$\beta$ conditions was not yet carried out. The clarification of the discrepancy is of high interest for theory and calculation methods.

### 3.4. Results of selected pre-calculations

A large number of pre-calculations were carried out for several supposed regimes of GDT-SHIP experiments. This was done to clear up which experimental regimes are best suitable for defined investigations of SHIP plasmas. Table 1 gives the parameters assumed for five proposed experiments and the results of ITCS computations. The calculation results are those achieved in steady state. In the regimes *v.2* and *v.5* the plasma in-stream was simulated as a time independent Gauss-like distribution $n_0(r)$ with a maximum of $5 \times 10^{13}$ cm$^{-3}$ and a half-width of 3.25 cm (see Fig. 3). The temperatures were fixed at $T_w$=$T_e$=100 eV. For the variants *v.1, v.3* and *v.4* real distributions of the plasma density and temperature appearing in the central cell of the GDT were used. The regime *v.1* is most similar to the first series of SHIP experiments with low NBI parameters. The other variants listed in Table 1 are considered as the most probable scenarios for future experiments. The injection power was 1 MW (*v.2*) and 2 MW (*v.3, v.4, v.5*), the injection energy – 20-25 keV, the duration of injection – 1 or 2 ms, neutral beam gases – H or D.

Table 1: Assumed parameters of proposed GDT-SHIP experiments and ITCS calculation results (bold highlighted).

| **Parameters** | ***v.1*** | ***v.2*** | ***v.3*** | ***v.4*** | ***v.5*** |
|---|---|---|---|---|---|
| Length, cm | 43 | 43 | 43 | 43 | 58 |
| Magnetic field (mid-plane/mirror), T | 2.4/5.2 | 2.4/5.2 | 2.4/5.2 | 2.4/5.2 | 0.7/2.5 |
| *Target plasma:* | | | | | |
| Electron temperature ($T_e$), eV | 60 | 100 | 80 | 80 | 100 |
| Unperturbed density ($n_0$), $10^{14}$ cm$^{-3}$ | 0.2 | 0.5 | 0.5 | 0.5 | 0.5 |
| Warm ion density ($n_w$), $10^{14}$ cm$^{-3}$ | **0.13** | **0.23** | **0.2** | **0.12** | **0.3** |
| Electron density ($n_e$), $10^{14}$ cm$^{-3}$ | **0.3** | **1.08** | **1.1** | **2.02** | **0.8** |
| *NBI System:* | H | H | H | D | H |
| Energy, keV | 17 | 20 | 25 | 25 | 25 |
| Total equivalent current, A | 13 | 50 | 80 | 80 | 80 |
| Injected power, MW | 0.2 | 1 | 2 | 2 | 2 |
| Duration, ms | 0.9 | 2(1) | 1.5 | 1.5 | 2 |
| *Fast Ions:* | | | | | |
| Maximal density ($n_f$), $10^{14}$ cm$^{-3}$ | **0.15** | **0.85** | **0.9** | **1.9** | **0.5** |
| Mean energy, keV | **7** | **9** | **10** | **9** | **12** |
| Total energy content ($W_f$), J | **8** | **43** | **81** | **166** | **120** |
| Trapped power, kW | **25** | **230** | **320** | **675** | **650** |
| Drag power, kW | **20** | **180** | **295** | **640** | **520** |
| CX-loss power, kW | **5** | **50** | **25** | **35** | **106** |
| Maximal local $\beta$, % | **1** | **8** | **8** | **15** | **62** |

Special interest consists in the experimental regime with a maximal fast ion density (*v.4*), in the comparison of H and D injection (*v.3* and *v.4*) and to achieve a maximal local $\beta$ parameter (*v.5*) for investigating high-$\beta$ effects in SHIP. Regime *v.1* is to represent the first series of SHIP experiments with low parameters both of target plasma and of NBI. Regime *v.2* should be the second step in the SHIP experimental program. Since the fast ion density had to be expected to achieve higher values, in the calculations of this regime the interest was focused on the iteration procedure between $n_f$ and $n_w$ in accordance with Eqs. (6, 7). The MCFIT calculations were performed up to 2 milliseconds after the NBI start. After four iteration steps the maximum of the fast ion density distribution remained in the range of the statistical error of a few per cent. The maximum of the fast ion density was calculated for $0.85\times10^{14}$ cm$^{-3}$ (see Figs. 3 and 4). Figure 8 shows the energy distribution of the fast ions for several time intervals. One can see that after 1 ms the energy spectrum varies very weakly in the low energy part only. The resulting mean energy is about 9 keV. The steady state spectrum having its peak at low energy of about 2 keV is the consequence of the increased electron density which causes a strong moderation of the fast ions. This energy spectrum and the high magnetic field result in a maximal fast ion $\beta$-value of merely 8 %.

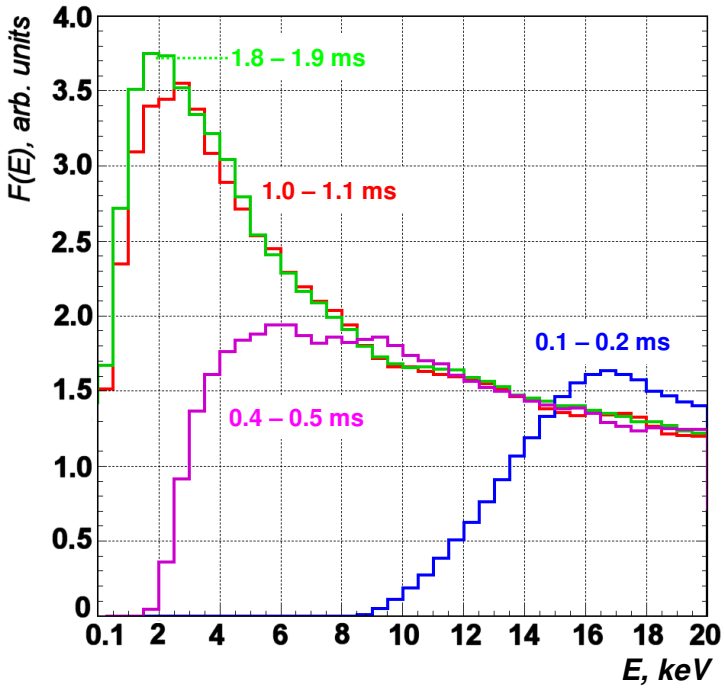


Fig. 8: Fast ion energy distribution in various time intervals (*v.2*).

Special MCFIT calculations were performed for regime *v.2* to determine the so-called fast ion energy and particle confinement time constants $\tau_E$ and $\tau_n$ in steady state, respectively. In the final iteration step, after reaching the steady state at the time moment of 1 ms the NBI was switched off and neutral gas, target plasma and background fast ions were hold in their actual states. Figure 9 shows the calculated relaxations of total energy content $W_f$ and of the total number of fast ions staying in SHIP. Fitting the drops of the energy and particle contents after 1 ms by exponential time functions gave the time constants of $\tau_E$=225 μs and $\tau_n$=550 μs. Regarding the

particle confinement time, the decay of the fast ion content after 1.6 ms is better fitted by the time constant $\tau_n$=270 µs.

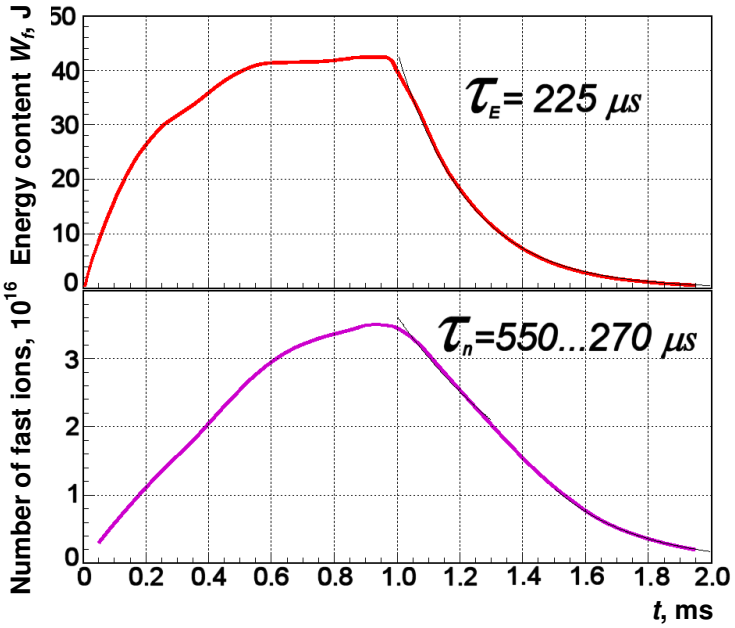


Fig. 9: Results of MCFIT calculation of fast ion energy and particle relaxation after NBI switch-off (*v.2*).

The variants *v.3* and *v.4* assume "realistic" profiles $n_0(r,t)$ and $T_e(r,t)$ of the target plasma column flowing into SHIP such as they were measured in previous GDT experiments. The values for target plasma density and electron temperature given in Table 1 are the maximum values that were reached during the shot. The new neutral beam injectors were modelled according to their projected parameters. Variant *v.3* was calculated with the injection of hydrogen beams with 2 MW injection power. One can see in Table 1 that the calculated fast ion parameters are close to those of regime *v.2* in which the NBI power is 1 MW only.

Regime *v.4* has the same input parameters as *v.3* but with deuterium beam injection instead of hydrogen. This scenario turned out to be the most preferable one regarding maximal fast ion density and energy content. Moreover, the injection of deuterium makes possible to measure fusion reaction products what gives additional diagnostic capabilities [14]. The ITCS calculations of this experiment showed that the total emission rate of DD-fusion neutrons will reach about $8\times10^{11}$ neutrons/s. The time dependencies of the main global fast ion parameters for this variant with deuterium NBI are shown in Fig. 10. It turned out, that the fast ion population reaches its steady state also very quickly, already in about 1.2 ms.

For regime *v.5* a maximal local $\beta$-value of 0.62 was computed. Compared with all other variants, it is the highest value. Therefore, in this variant the new ITCS modules were used for the numerical study of high-$\beta$ effects in SHIP (see also 3.1.3.). The predicted results of high-$\beta$ distortion of the magnetic field were presented in Fig. 6. The fast ion density in this regime remains relatively low, mainly because the high-energy ions injected by the NBI move with a large gyro-radius in the magnet field with

substantially reduced strength. A part of them is even lost to the chamber wall. So, the high value of $\beta$ is more the result of the low magnetic field but, unfortunately, not of high fast ion density. Even so, this scenario is recommended for the study of high-$\beta$ effects and for the search for $\beta$-limits of stability of two-component plasmas confined in axial-symmetrical gas dynamic traps.

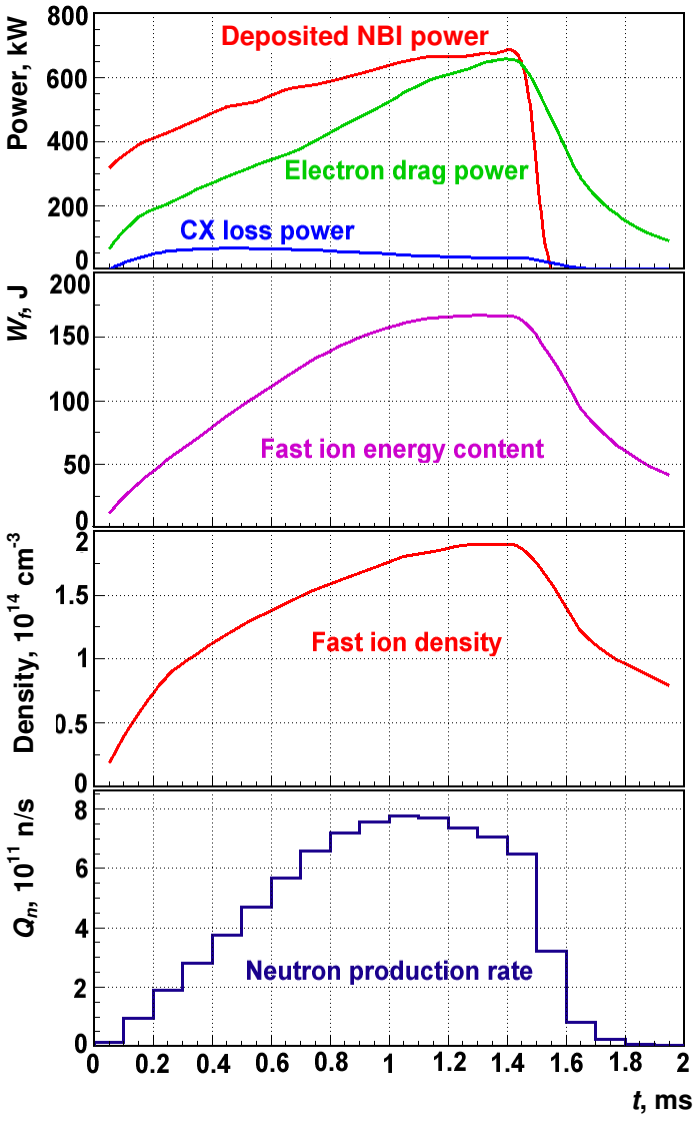


Fig. 10: Calculated time evolutions of global fast ion parameters in regime *v.4*.

### 3.5. Conclusions from pre-calculations

From the results of pre-calculations the following conclusions could be drawn:

- The Monte Carlo fast ion transport code MCFIT has been modified and extended to be able to consider non-linear processes that are expected to be significant for the phenomena which could occur in SHIP plasmas. After that, it was used to study certain possible experimental scenarios.

- The new code NEUFIT was developed for the calculation of the neutral gas inside the SHIP chamber and then was used for numerical simulations together with the MCFIT code.
- The simulation of a 2 MW NBI power regime with hydrogen injection gave a maximal fast ion density of about $10^{14}$ $cm^{-3}$ with a mean energy of 10 keV.
- The calculation of the deuterium injection regime with 2 MW NBI power gave the maximal fast ion density of $1.9\times10^{14}$ $cm^{-3}$ with the mean energy of 9 keV. This value of the fast ion density is already relevant for a GDT based neutron source. The total neutron production rate in this experiment was calculated to reach about $8\times10^{11}$ neutrons/s.
- The calculation of an experimental scenario with reduced magnetic field resulted in a maximal $\beta$-value of 0.62. Therefore, this regime is recommended for the study of high-$\beta$ effects in two-component plasmas confined in axial-symmetric mirrors.

## 4. Theory and numerical simulations of self-organizing processes in two-component plasmas

### 4.1. Two-dimensional dynamics of two-component plasma with finite $\beta$

A particular interest in studying the dynamics of two-component plasma was caused by recent experimental results obtained in GDT experiments in which fast ion pressure was comparable with the magnetic field pressure, i.e. $\beta$ near to 1. It was observed that the fast ions gathered in the near-axis region in time much shorter than the collision time. This phenomenon is outside the scope of classical plasma physics and, hence, is not reproduced by the MCFIT code. Simple estimations show that three-dimensional (3D) effects, like resonances of bounce oscillations with azimuthal drift rotation and ballooning perturbations can be significant for the two-component plasma dynamics in GDT experiments under high-$\beta$ conditions. Such effects could occur in high-$\beta$ experiments planned for SHIP too. However, the two-dimensional problem itself considered in Ref. [15] appeared to be quite interesting. Therefore, in the project its theoretical analysis was continued to identify and understand the mechanism of the observed effect in more detail. The theoretical studies were supported by two-dimensional numerical simulations with a particle-in-cell (PIC) code.

The goal was to studying two-component plasma dynamics in the framework of simple theoretical formulation. To this end, following presuppositions were made. Cold and collision-less plasma contains a small admixture of fast ions with the Larmor radius comparable with the transverse size of plasma. The fast ion component has a finite pressure $P_f$ satisfying the condition

$$\beta << 1 , \tag{8}$$

where $\beta$ is defined by Eq. (1). By this approximate assumption, in the theoretical considerations terms $\sim\beta^2$ were neglected if terms $\sim\beta$ were present. All quantities depend only on co-ordinates transverse to the magnetic field which is directed in $z$-direction. The characteristic time of the considered processes is assumed to be much

larger than the ion cyclotron time. Therefore, we used the adiabatic conservation of fast ion magnetic moment $M \cong E_{f\perp}/B$, where $E_{f\perp}$ is the kinetic energy of their transverse movements. Also, the characteristic time is assumed to be much larger than the time of fast magnetic sound propagation in plasma across the magnetic field, and the fast ion velocity is of order or less than the electron thermal velocity. Finally, for simplicity, all fast ions are assumed to have equal magnetic moment. In the outlined framework of approximations the following picture of the self-organizing effect was obtained.

The magnetic moment conservation makes some properties of the considered plasma unexpectedly different from the properties of collision plasmas. The ensemble of ions with large Larmor radii has the potential energy of interaction caused by the magnetic field perturbation produced by these fast ions themselves. The potential energy is the sum of the fast ion energy and magnetic field energy and it is uniquely defined by the spatial distribution of their guiding centers (therefore, this energy is denoted as “potential energy”). Although, the proper magnetic energy increases when the fast ion guiding centers come closer together, nevertheless, due to the magnetic momentum conservation, the total potential energy reaches its minimum when the guiding center spatial distribution is maximally compact.

The guiding center velocity field is incompressible, which restricts the compacting of the fast ions. Any non-uniform distribution of the fast ions causes their gradient drift by the $\vec{B}\times\nabla B$ force. If the equilibrium with the immovable cold component corresponds to a minimum of the potential energy (taking into account the incompressibility) then the equilibrium is stable. Otherwise, instability of non-uniform gradient drift evolves.

There is an interaction between the dynamics of the fast ions and the cold plasma component. The change of the fast ion charge distribution causes a change of electric field, which accelerates the cold component in such a way that the polarization current compensates the charge density change. This interaction results in excitation of $\vec{E}\times\vec{B}$ turbulence. The growing kinetic energy of the cold plasma motion comes from the fast ion potential energy. Therefore, this process is accompanied by a self-localization of the fast ions, i.e., by transition to a more compact guiding center spatial distribution. This effect is opposite to the usual tendency of collision plasmas to spread out across the magnetic field due to diffusion and instabilities.

We also considered the dynamics of two-component plasma containing two sorts of ions, the cold ions with zero magnetic moment and a small admixture of fast ions with fixed magnetic moment *M*. In this dynamics, the roles of the components are clearly separated: the cold component carries the kinetic energy of $\vec{E}\times\vec{B}$ motion and the fast component carries the potential energy which is the sum of fast ion energy and magnetic field energy. If the magnetic moment *M* conserves, the potential energy is minimal for the maximally compact spatial distribution. The compacting is restricted by the Liouville theorem providing that the drift motion is incompressible.

The two-component magnetic moment distribution assumed in the preceding simplified model is not of fundamental importance, but simplifies the calculations only. The consideration can be generalized to plasma containing the ions with an

arbitrary magnetic moment distribution. Supposing that the initial level of $\vec{E}\times\vec{B}$ turbulence is low and the spatial distribution of the guiding centers is such that the Liouville theorem permits transition to a more compact distribution with the smaller potential energy. Then, a redistribution of energy over degrees of freedom has to take place. It has to be accompanied by an increase in the proper magnetic energy and spatial localization of a fraction of ions carrying the main part of the potential energy. Only the conservation of the magnetic momentum for sufficiently long time inversely proportional to $\beta$ is important. Therefore, the discussed phenomena can be of interest from the viewpoint of a wide class of collision-less problems in plasma physics and astrophysics, where the magnetic moment conservation is valid for a sufficiently long time.

### 4.2. Three-dimensional dynamics of two-component plasmas

The plasma in GDT experiments shows unique properties which make the research projects connected with this facility more attractive. Specific plasma properties in these experiments are caused by the fact that the fast ion pressure is comparable with magnetic field pressure and the fast ion gyro-radius is comparable with the plasma radius. Experiments showed, that under these conditions the fast ions gather in narrow stable formation localized near the device axis during a time less than the collision time. Theory which analyzes the phenomena involved in two dimensions proofs the fact that under the conditions of magnetic moment conservation such a formation just corresponds to the minimum of total energy [15]. However, in the case of monotonically decaying radial profile the radial localization is impossible in the frame of the 2D-model, because of phase volume conservation. Such a prohibition is absent in a 3D-model. Therefore, the study of the 3D-problem causes special interest and was started within the joint project.

In the three-dimensional problem resonances between bounce oscillations and azimuthal rotations play an important role. The ions moving along the resonance trajectories accumulate radial displacement caused by magnetic field asymmetries. On the other hand, their displacement causes changes of the field asymmetry. Investigation of such self-consistent problems is in progress. There is a simpler problem where “test” particle transport in the field, which is perturbed by “field” particles, is studied. This problem was investigated in detail in the project and the results are prepared for publication. Subsequently, a more detailed description of the analyzed non-self-consistent problem and some results are presented.

The most important resonances take place if the ratio of azimuthal and bounce frequencies $\omega_\varphi / \omega_z$, is a rational number *m/n*, where integers $m$ and $n$ are comparable with unity. The simplest estimation for resonance frequencies is

$$\omega_\varphi \le v\rho\beta / a^2 \quad , \quad \omega_z \sim v / L, \tag{9}$$

where $v$ and $\rho$ are the fast ion velocity and gyro-radius, $a$ and $L$ are the plasma radius and length, respectively. $\beta$ is defined by Eq. (1). Hence, the simple criteria of low order resonance existence can be written in the form

$$\beta > \frac{a^2}{L\rho}. \tag{10}$$

The GDT-SHIP experiment parameters satisfy this condition in high-$\beta$ regimes. Here, the resonances play a double role. First, the fast ions moving along resonance trajectories return to the same point after many oscillations, while non-resonance trajectories sweep a surface in the phase space. Therefore, just the resonance "field" particles, that have been asymmetrically injected, keep this asymmetry and cause the magnetic field asymmetry. Second, the resonances provide a mechanism of enhanced stochastic transport of the "test" particles. Small perturbations of the magnetic field separate the ion trajectories into two categories - "passing" and "trapped" trajectories [16]. "Passing" trajectories are those, the cross-points through a section $z$=constant (Poincare section) of which form a curve which bypasses the system axis. However, the corresponding curves of "trapped" particles are localized in small islands located around staying points on the resonance surfaces. The curves of both types of trajectories on a Poincare section are separated by a separatrix line which is surrounded by a stochastic layer. Larger perturbations result in resonance islands which are overlapping, if the resonance island size exceeds the inter-resonances distance. In this case, an ion can move a rather long distance in radial direction.

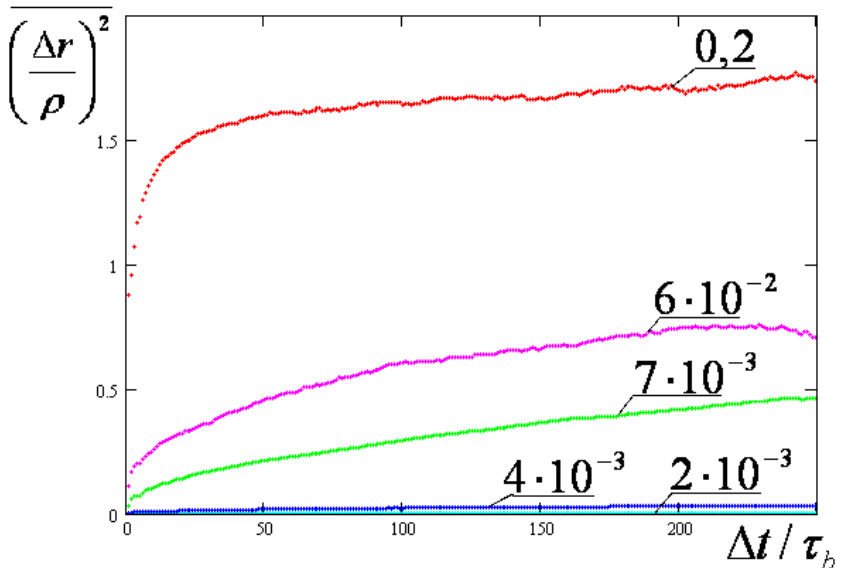


Fig. 11: Dependencies of the mean squared radial displacement normalized by gyro-radius on time normalized by the mean bounce time for different values of the relative magnetic field perturbation $\langle \Delta B / B \rangle$.

In order to study this stochastic transport, the first version of a special 3D-code has been developed. By means of this code, first, the magnetic field perturbations caused by non-symmetric neutral beam injection were calculated and second, the "test" ion motion was simulated. In Fig. 11, examples of dependencies of fast ion mean squared radial displacements on time are shown for different levels of magnetic field perturbations. The main result obtained from this study is that the significant stochastic transport is possible provided the relative field perturbation exceeds $\langle \Delta B / B \rangle$~0.03. However, the numerical results also show that the existent asymmetry of the GDT neutral beam injection cannot provide such a level of field perturbation. Hence, further research is necessary to clarifying the self-organizing

effect of the fast ions which were experimentally observed in GDT high-$\beta$ experiments.

## 5. Results of GDT-SHIP experiments and ITCS/MCNP calculations

### 5.1. Experiments with moderate parameters

After an extensive test phase, the first series of research experiments at the GDT-SHIP facility was started in December 2005. These experiments were carried out with moderate parameters both of target plasma and of neutral beam injection. The parameters of the target plasma influx were: Plasma radius ~5 cm, on-axis density ~$10^{13}$ cm$^{-3}$ and the electron temperature $T_e$ was 65 eV. Two injectors delivered a total beam current of 15 Amperes of hydrogen atoms with an energy of 16 keV in a pulse with duration of 0.8 milliseconds. The total injected energy was ~200 J of which ~20 J were deposited in the plasma by ionization. The experimental regime of this series of measurements is approximately modeled in the ITCS calculations for regime *v.1* which is included in Table 1. In the following, the most important results will be presented and commented.

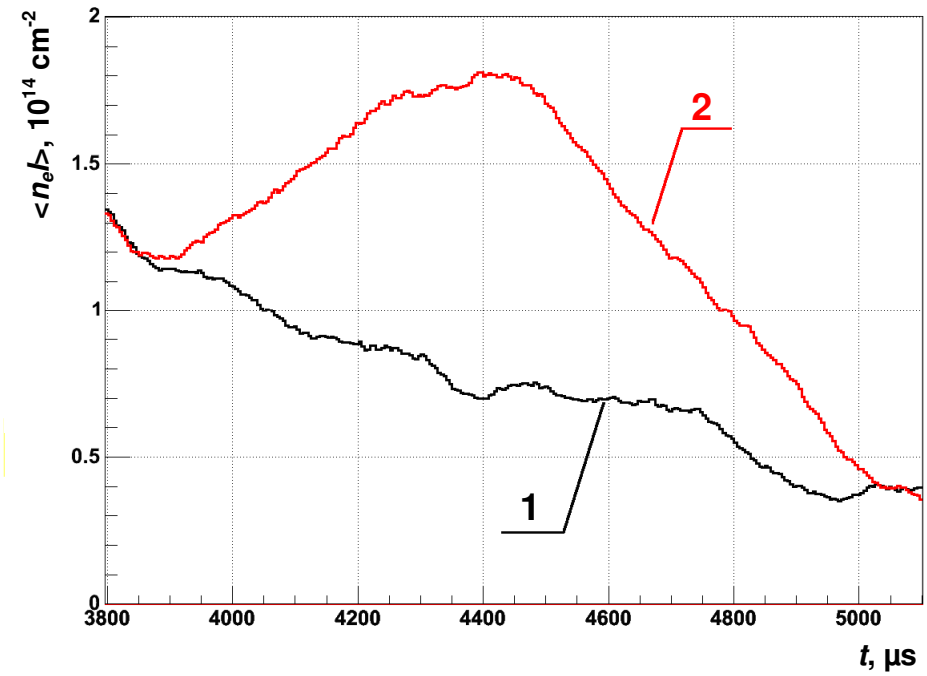


Fig. 12: Time evolutions of line-integrated electron density in the centre of SHIP during shots without NBI (1) and with NBI (2).

Figure 12 shows signals of the line-integrated (along the plasma diameter) electron density $<n_e l>$ (alternatively also called "linear density") such as it was recorded by the $CO_2$ dispersion interferometer in the centre of the SHIP cell. The growth of the line-integrated density during the NBI indicates the build-up up of the fast ion density. The maximum of signal 2 amounts to $<n_2 l> \cong 1.8\times10^{14}$ cm$^{-2}$. At the same time moment (~4450 µs) signal 1 gives about $<n_1 l> \cong 0.8\times10^{14}$ cm$^{-2}$. The letter quantity is just the line-integral of the "unperturbed" density $n_0$ of the plasma influx which was introduced in subsection 3.1.1. Considering the relations between the various particle densities

governed by Eqs. (6, 7), one gets from these values the estimates of line-integrals of the "warm" ions $<n_w l>\cong 0.4\times10^{14}$ cm$^{-2}$ and of the fast ions $<n_f l>\cong 1.4\times10^{14}$ cm$^{-2}$ at this time moment. Hence, comparing both cases one can conclude from these measurements that in the case with NBI switched-on the mean value of the fast ion density is two times higher than that of the target plasma influx and three times exceeds the density of the warm ions.

The spatial fast ion profile measured by the imaging charge exchange atom analyzer is shown in Fig. 13. The profile is normalized to the value of the fast ion linear density $<n_f l>=1.4\times10^{14}$ cm$^{-2}$ which was derived from the dispersion interferometer measurements. The characteristic dimensions of the fast ion plasmoid (referring to the 1/e-level of density) are: Axial length 5 cm and diameter 13 cm. The average energy of fast ions was determined to be 6 keV and the maximal density value amounts to $1.2\times10^{13}$ cm$^{-3}$ [17].

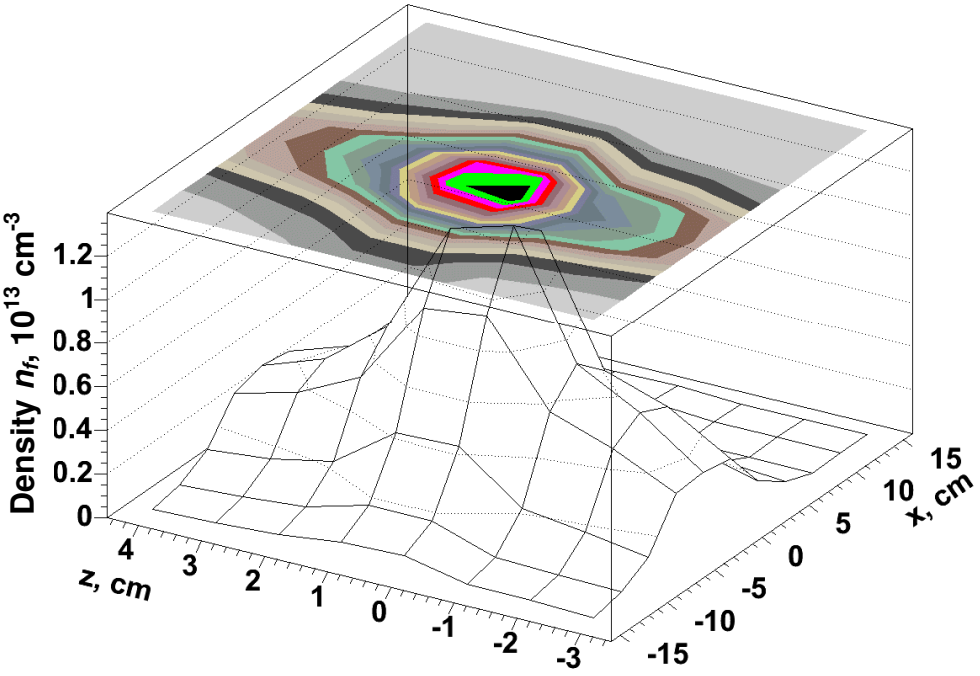


Fig. 13: Two-dimensional representation of the spatial profile of fast ion density at time moment of maximal energy content.

The important conclusion, which could be drawn from these measurements, follows from the axial extension of the plasmoid. It corresponds to the value which is determined by the initial angular divergence of the injected beams alone. This result evidences the fact that there is no enhanced scattering of the fast ions which would contribute to the broadening of their axial density profile. Moreover, the contribution from collisions with warm and fast ions is really small in these low-parameter experiments.

The diamagnetic perturbation of magnetic field $\Delta B$ was measured by MSE diagnostics [18]. A maximal value of the relative distortion $\Delta B/B_{vac}$ of merely 2 % was measured.

The time evolution of the total energy content of the fast ions was measured by means of a diamagnetic loop. The results of the measurement and of the corresponding ITCS calculation are shown in Fig. 14. All other computed parameters are also in good agreement with measurement results.

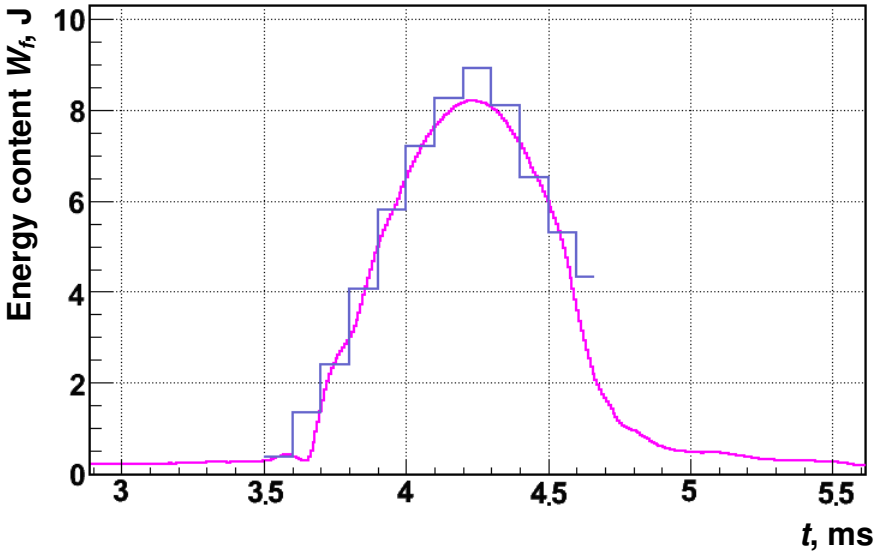


Fig. 14: Time evolution of fast ion energy content $W_f$:
Smooth line – measurement, histogram – ITCS.

The first series of GDT-SHIP experiments together with corresponding ITCS computations could be assessed as follows:

- The highlight was the successful synthesizing of the fast ion plasmoid such as it had been proposed. Even with low parameters of target plasma and of neutral beam injection, the fast ion density was three times higher than that of the warm ions of the target plasma. Results of pre-calculations with ITCS codes for an experimental regime being close to that, which was afterwards actually realized, were in good agreement with the measurements.

- The maximal fast ion density which was achieved in experiments amounted to $1.2\times10^{13}$ $cm^{-3}$. About the same value has been reached in the end cells of the famous TMX tandem mirror experiment already in the eighties, however, with the utilization of a ten times higher injection power [19].

- The plasma composition consisting of the fast ion plasmoid and of the target plasma turned out to be stable. No indications of any MHD-instabilities of the whole plasma and of micro-fluctuations caused by the fast ion plasmoid were observed. The good agreement of the measurements with the results of ITCS simulations confirms the validity of the classical plasma physics. The fast ion confinement was definitely determined by Coulomb collisions and charge-exchange reactions.

## 5.2. Experiments with enhanced parameters

A new power supply for the whole NBI system at the GDT-SHIP facility was installed in 2007. After this, the first series of research experiments with enhanced parameters could be carried out. The relevant parameters were as follows. The target plasma density was practically the same as in the first series about $10^{13}$ cm$^{-3}$, however, it was heated-up to an electron temperature of about 100 eV. The most substantial improvement came from the new injectors at SHIP: They injected hydrogen beams of total power approaching 1 MW with pulse duration up to 4 milliseconds. The energy of the injected atoms was in the range between 20 and 25 keV. The diameters of the beams were about 9 cm in their focus points. The power density of the deposited (ionized) neutral beam power amounted to about 20 kW/cm$^3$.

Figure 15 shows the time evolutions of the linear electron density measured with the dispersion interferometer in the mid-plane of SHIP in two cases: Without NBI (1) and with maximal NBI power (2).

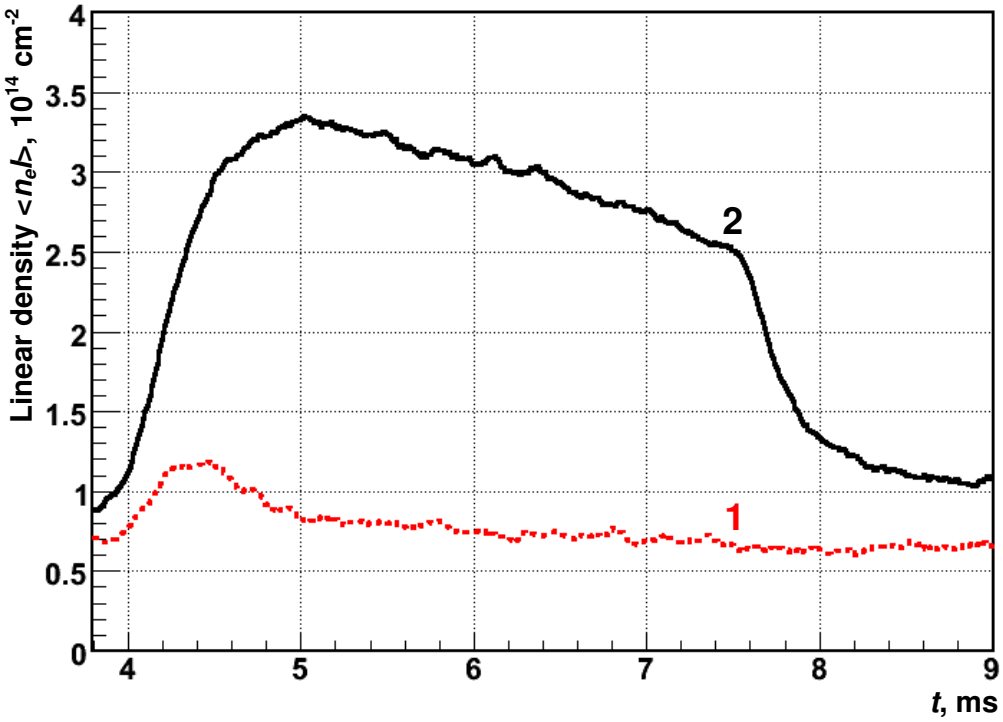


Fig. 15: Time evolutions of line-integrated electron density in the centre of SHIP during shots without NBI (1) and with NBI (2).

The effect shown in Fig. 15 is the same as represented in Fig. 12 of section 5.1., but it is essentially stronger shaped: The substantially higher electron density in case with NBI indicates the presence of the fast ion plasmoid. According to the larger difference between the signals, the density of the plasmoid should be higher. The analysis made analogously to that of section 5.1. gives the following densities in the time moment when the maximal fast ion density appears: Density of fast ions $n_f \cong 4\times10^{13}$ cm$^{-3}$, density of target plasma ions $n_w \cong 0.3\times10^{13}$ cm$^{-3}$, density of target plasma influx $n_0 \cong 10^{13}$ cm$^{-3}$. These data illustrate that the fast ion density exceeds four times the density of the target plasma influx and is even more than one order of

magnitude larger than the warm ion density. The mean energy of the fast ions turned out to be about 15 keV. The analysis of the spatial profile of the fast ion density gives the characteristic dimensions (1/e-level) of the plasmoid: The length is about 4 cm and the diameter about 15 cm.

The figure which should be highlighted is the high value of the averaged fast ion density $n_f \geq 4\times10^{13}$ cm$^{-3}$ which is more than three times higher than that achieved by the TMX experiment by utilizing neutral beams with a power four times larger than in this SHIP experiment.

The physical effect of the ambipolar potential which is built-up by the fast ion plasmoid was discussed in subsection 3.1.1. It was already observed in the experimental series with low parameters (see Fig. 12 in section 5.1.). It had to be expected essentially higher in experiments with enhanced parameters. In addition to measurements of the linear electron density $<n_e l>$ in the mid-plane of SHIP, the plasma outflow was measured in the expander cell just beyond the last mirror coil. Figure 16 shows the results for two cases: Without NBI (1) and with NBI (2). Both curves show that the plasma outflow is reduced by about a factor four if the NBI into SHIP is switched-on. This is the effect of the ambipolar potential of the fast ion plasmoid which expels the target plasma ions. Therefore, the target plasma outflow from the central cell through SHIP into the expander cell is decreased and hence the quality of plasma confinement in the central cell is substantially improved. This positive effect of a sufficiently strong ambipolar potential, which is called ambipolar plugging, is already known from the development of tandem mirrors like TMX and GAMMA-10 [20], however, it was the first time experimentally demonstrated in a mirror facilitiy of gas dynamic trap type.

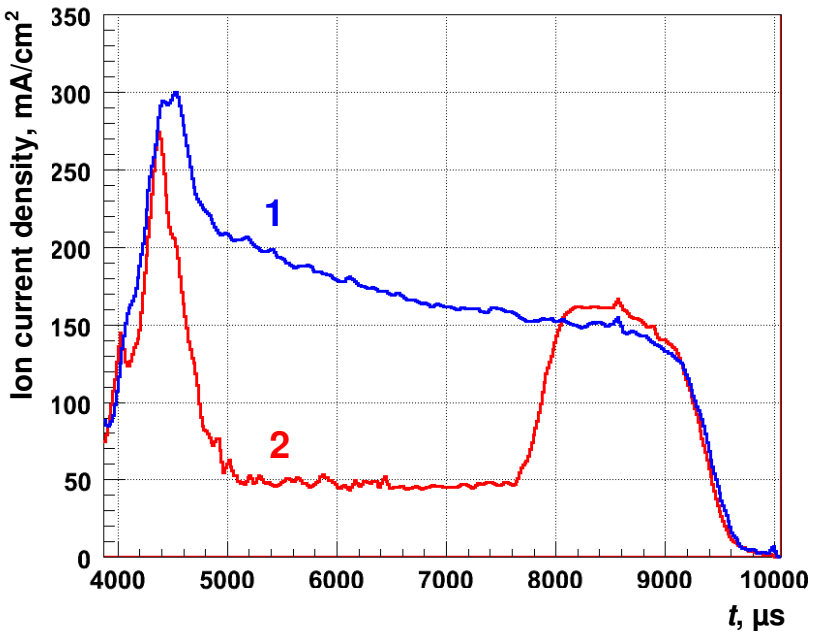


Fig. 16: Time evolutions of ion current density of plasma outflow into the expander end cell for two cases: Without NBI (1) and with NBI (2).

A subset of experiments was carried out with varying NBI power. Figure 17 shows calculated and measured values of maximal fast ion densities appearing in courses of the shots in dependency on the pulse averaged deposited power $\overline{P}_{dep}$. The agreement is very good. The maximal deviation is less than 15 %. The departure from the proportionality of both quantities shows that with a stronger source of fast ions their probability of particle loss is increasing. The classical causes of this effect are charge exchange at gas atoms and angular collisions with ions which then result in increasing the particle outflow through the mirrors. The analysis of the situation which is simulated by MCFIT reveals that the non-linear collisions between fast ions are the decisive cause of the observed dependency.

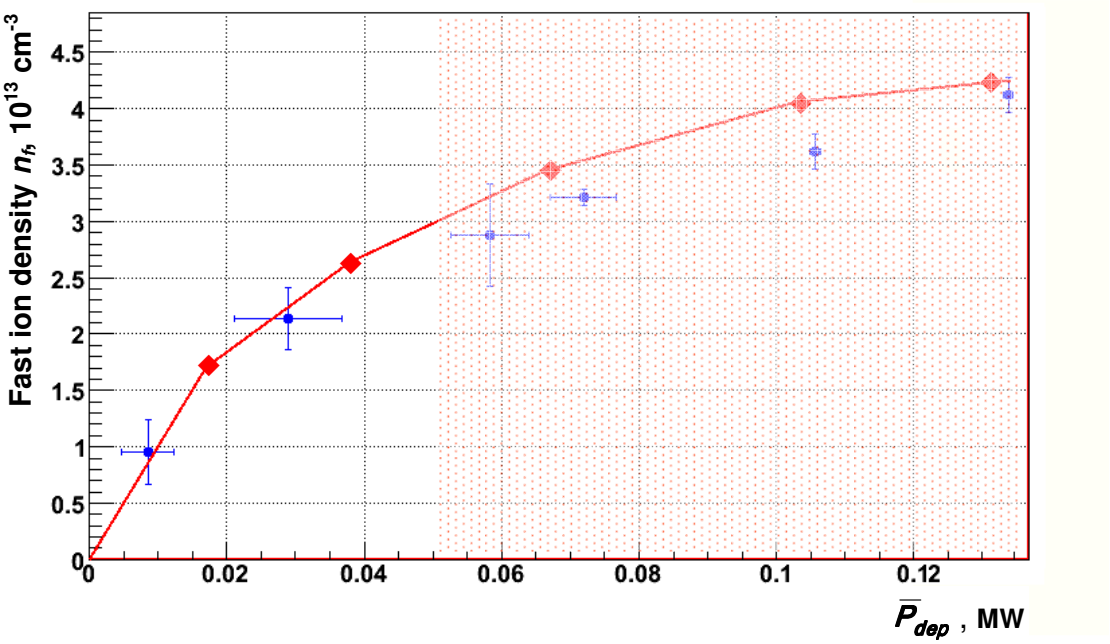


Fig. 17: Measured (cross-points) and calculated (rhombi) maximal values of fast ion density in experiments with various NBI power.

From the good agreement between the results of ITCS computations and measurements which is demonstrated by Fig. 17, one could conclude the validity of the classical plasma physics for this set of experiments with enhanced parameters. This is obviously justified if looking on the balance of fast ions only. However, in the four experiments with higher NBI power lying inside the marked area of the diagram, a special radio-frequency Longmuir probe displayed high-frequency electro-magnetic oscillations the amplitude of which increased with the density build-up of the fast ion plasmoid. The main frequency of the fluctuations is about 37 MHz which corresponds to the ion-cyclotron frequency in the mid-plane of SHIP. Similar oscillations had been observed in special experiments at TMX and GAMMA-10 if plasma compositions with strongly anisotropic ion velocity distributions had been studied. They have been identified as so-called Alfven ion-cyclotron (AIC) micro-instabilities. In case of SHIP one could assume that these are connected with certain types of motion of the fast ion plasmoid as a whole.

According to actual theory, the AIC-oscillations develop provided the parameter product $\beta \cdot A$, where $A = \langle E_\perp \rangle / \langle E_\parallel \rangle$ is a parameter characterizing the anisotropy of the plasma velocity distribution, approaches unity. $E_\perp$ and $E_\parallel$ are the kinetic energy of the particle motion perpendicular and parallel to the magnetic field $\vec{B}$, respectively. In the SHIP experiment in which the first time the oscillations were observed both parameters had the values $\beta \cong 0.02$ and $A \cong 35$, so that with $\beta \cdot A \cong 0.7$ the observation may be interpreted to be consistent with the theoretical prediction of the threshold. Theoretical work for detailed investigation of the findings was started in BINP.

Considering the fact that in case of the four SHIP experiments in which fluctuations were observed (see Fig. 17), the fast ion confinement is still very well described by ITCS computations based on classical plasma physics, one must conclude that the oscillations are not yet strong enough to distort the fast ion velocity distribution to that degree which would result in increased fast ion losses. This conclusion is also supported by the measurements with the imaging charge exchange atom analyzer carried out at these experiments. They did not show an axial broadening of the fast ion density peak which would indicate the presence of additional angular scatterings caused by micro-fluctuations.

The series of experiments with enhanced parameters together with corresponding ITCS computations could be assessed as follows:

- For the first time, the effect of ambipolar plugging was demonstrated in a mirror facility of gas dynamic trap type.

- With increasing NBI power the appearance of high-frequency electro-magnetic oscillations was observed. Surprisingly, they did not show any degradation of the fast ion confinement which remained such as determined by classical plasma physics.

- This “co-existence” of plasmoid oscillations and classical fast ion confinement survived with further increase up to 0.9 MW of NBI power resulting in the record value of the fast ion density $n_f \cong 4.2 \times 10^{13}$ cm$^{-3}$.

- The full clarification of the nature of the oscillations and the search for possibilities of their damping or even of prevention needs theoretical investigation and new experiments with further increased NBI power.

### 5.3. Test experiments with deuterium injection and neutron transport calculations with MCNP

Within the framework of the joint research project, first experiments with the injection of deuterium were carried out. The main purpose of the experiments was the testing of the new injectors for the injection of deuterium and the testing of the neutron measurement technique which is presently available. Research experiments which are planned in the SHIP research program (see section 3.4.) will be carried out in the next experimental phase of GDT-SHIP. In parallel, neutron transport calculations with the Monte Carlo code MCNP using the neutron data library ENDF/B-VI.8 [8] were prepared and test calculations carried out. Unfortunately, the neutron detectors were not yet calibrated so that measurement and calculation results could not be

compared. Nevertheless, the model calculations and a few results obtained should be briefly presented.

The geometry of SHIP was modeled by the simple cylindrical model shown in Fig. 18. Only the SHIP container and both mirror coils are involved in the model. Some thin structure elements inside of the container and several elements outside are not yet included. If necessary, they can be easily introduced. As example, neutron fluxes were calculated at three detector positions (D1, D2, D3) which are in realistic radial distance from the axis.

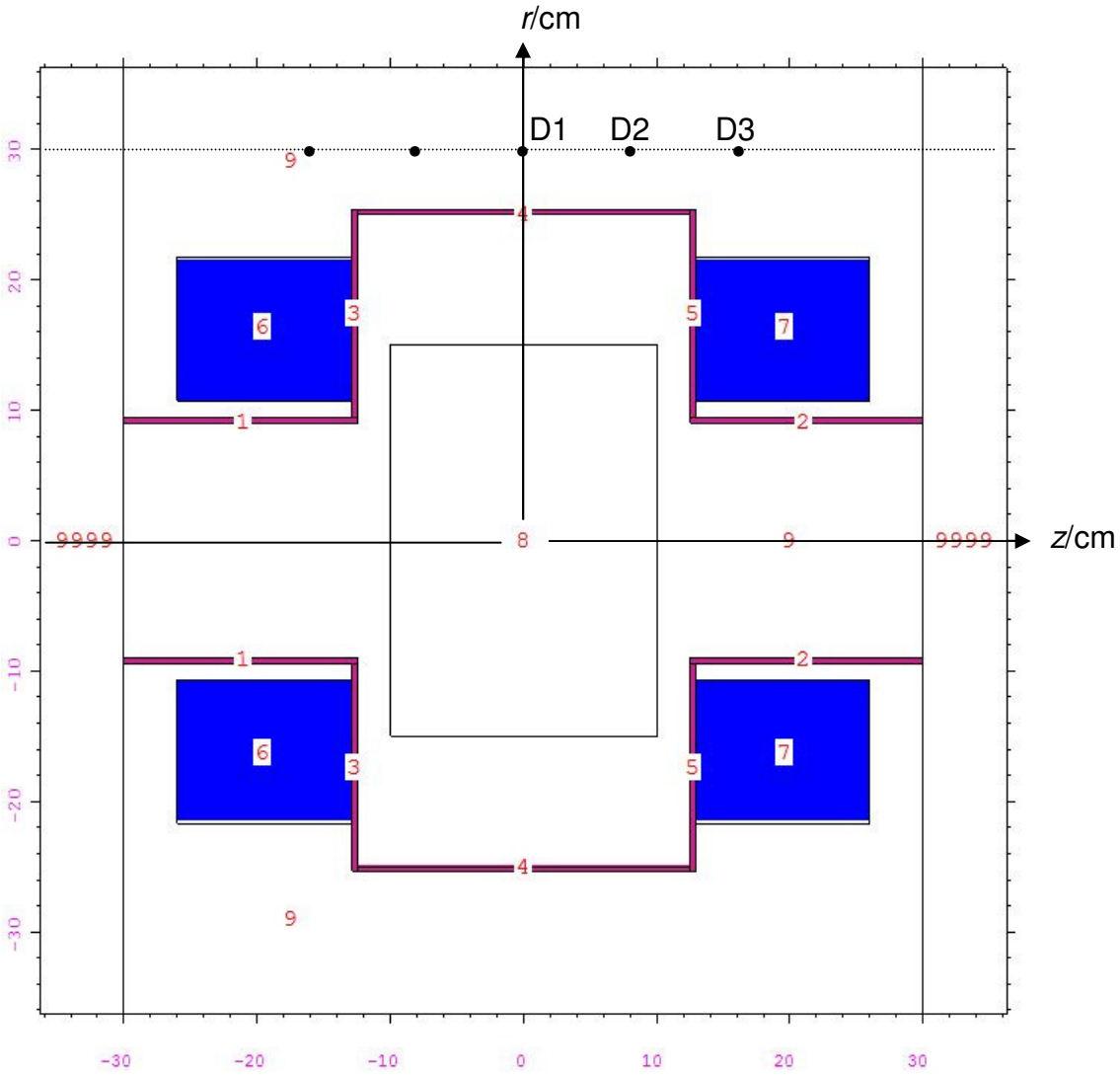


Fig. 18: Axial cross-section through MCNP geometry model of SHIP with possible detector positions indicated.

In addition to the modeling of the geometry that of the neutron source is essential too. Here, the description of its spatial distribution is the crucial point. It must be calculated from the fast ion density distribution, which is delivered by MCFIT, by means of the auxiliary code MAXIM or it must be approximately constructed from information derived from measurements. MCNP offers the user to representing the source as a disk with a density distribution described by Gaussians along the *z*-axis

and in radius. The user must input the values of the so-called FWHM´s (full width at half maximum). In this way, the density distributions of the fast ion plasmoids should be described in sufficiently good approximation. In the test calculations the following values of the FWHM´s were used: 8.326 cm for radius and 3.330 cm for *z*. In addition, in the MCNP simulation the extension of the source was limited to the volume inside cylinder number 8 indicated in Fig. 18.

There are no problems with the modeling of the energy and the flight direction of a starting fusion neutron: In-built options of MCNP offer the user to fix the start energy (here 2.45 MeV) and to order isotropic distribution of the flight directions.

The test calculations with MCNP were carried out with the described models of geometry and source. The calculated neutron fluences (per pulse) are shown in Fig. 19. The values are normalized to the total number of neutrons, which were released from DD-fusion reactions during a pulse, of $1.30\times10^{8}$. According to information from the GDT team, this was a realistic estimate for the scheme realized in the test shots. The portion of so-called “uncollided” neutrons is given separately. “Uncollided” neutrons are those which arrive at the detector without any collisions. One can see that even in the central detector position about one third of the neutrons suffered scatterings in the coils and/or in the container wall. Moreover, the stronger drop of the fluence from D2 to D3 illustrates the impact of a partial screening of position D3 by the coil.

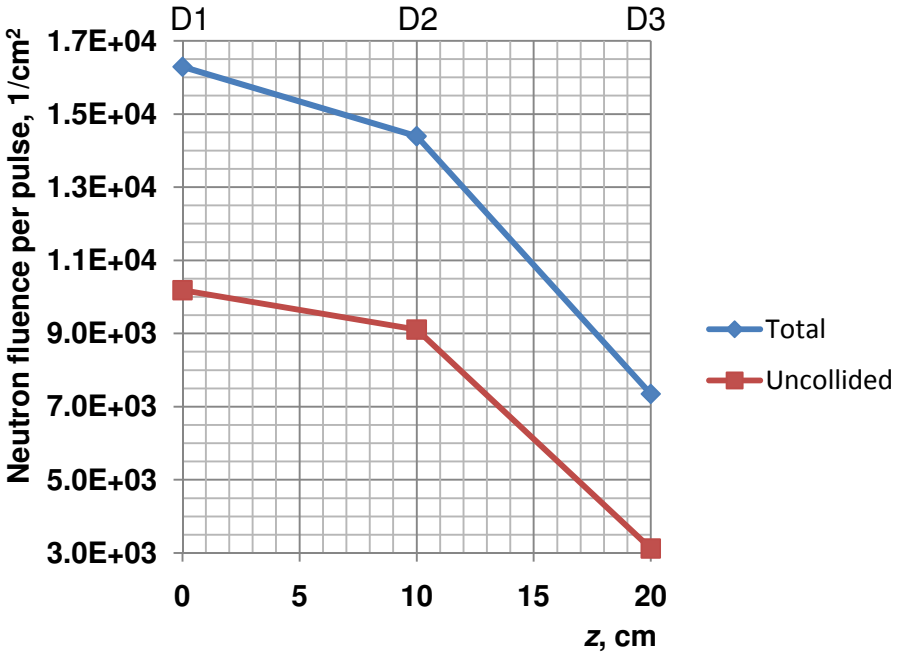


Fig. 19: Calculated total and “uncollided” fluences normalized to the total neutron emission of $1.30\times10^{8}$ per pulse.

The energy spectrum of the neutron fluence is of importance for the analysis of the neutron measurements. In any case, the final signal of a detector is the convolution of its so called response function, which generally depends on the neutron energy, with the energy spectrum of the neutron fluence. Depending on the quantity which should be determined by the neutron measurements, the type of neutron detector

must be chosen. To support this analysis, the fluence spectra were calculated at the selected detector points. Figure 20 shows the results in form of histograms. The histogram values are the fluences which are integrated over the energy interval belonging to. An interval width of 0.1 MeV was chosen. One can see that the spectra at both central positions D1 and D2 do not considerably differ however a noticeable deviation appears for D3 and this both in the highest energy interval in which the uncollided neutrons are collected and in the energy part below the DD-fusion peak in which the scattered neutrons are collected.

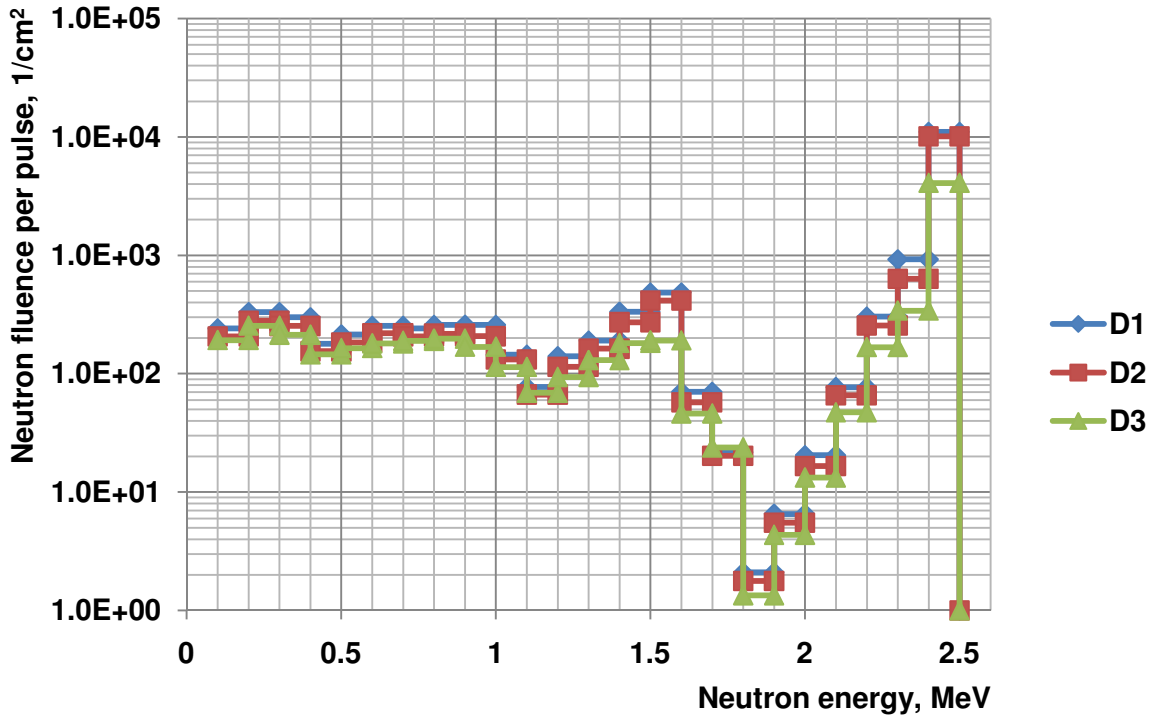


Fig. 20: Calculated energy spectra of neutron fluences.

In addition, time-dependent neutron transport calculations were carried out for a realistic model of a time-dependent neutron source reflecting the build-up and the decay of the fast ion plasmoid. From the results obtained, the conclusion could be drawn that there is practically no retardation between the source and the neutron field at the selected detector positions which could be of relevance for the planned neutron measurements.

Regarding the calibration of the neutron measurement technique at SHIP, one possibility could be the following: On the one hand, one should have a well defined and well measured experiment with deuterium injection. On the other hand, the neutron source distribution appearing in this experiment should be calculated as accurate as possible with help of the ITCS. After this, the neutron fluences at selected detector positions should be calculated with MCNP. From calculations and measurements the relations between detector signal (measured) and both the neutron fluence at detector position and the total number of fusion neutrons released during the shot (both quantities computed) could be established. With the results of the same procedure for a second experiment with another injection power the

proportionalities between detector signal and neutron fluence/number of fusion neutrons produced should be verified.

## 6. Summary and main conclusions

The investigations done within the framework of the joint research project yielded a great number of new findings. The highlights of the research can be summarized and the most important conclusions can be drawn as follows:

1. To prepare the ITCS (Integrated Transport Code System) for computations of plasma phenomena which were expected to occur in course of SHIP experiments, it had to be extensively modified and extended: The Monte Carlo fast ion code MCFIT was modified to be capable to consider several non-linear processes which should be significant in SHIP plasmas. The deterministic neutral gas code NEUFIT was newly developed from a preceding code to allow more realistic descriptions of the SHIP geometry and of the gas-wall interactions. Non-linear effects were considered by iterative calculations of these two codes between which the necessary data preparations and transfers are accomplished by means of some auxiliary codes. The iterative computation scheme was extensively used for SHIP plasma simulations within the framework of classical plasma physics.

2. Before the start of SHIP experiments, with help of ITCS calculations certain experimental scenarios were studied to get information on the type of plasma states which can be realized in SHIP and on parameters which can be achieved provided that classical plasma physics remains valid. In this way, advices on the first two series of experiments with hydrogen injection were derived. Moreover, the results revealed that for maximal fast ion densities the use of deuterium neutral beams is favorable and that a maximal value of plasma $\beta$ around 0.6 can be achieved in the case of low magnetic field which can be realized by increasing the distance between both mirror coils.

3. The first series of research experiments was carried out with relatively low density and temperature of the target plasma, with total beam power of merely 0.23 MW and pulse duration of 0.8 ms only. In spite of low parameters, the fast ion plasmoid was synthesized and its density turned out to be three times higher than that of the target plasma ions. A maximal fast ion density of $1.2 \times 10^{13}$ $cm^{-3}$ was achieved. Such a density had also been obtained at the famous TMX facility in the eighties, however, with a ten times higher injection power [18]. No indications for any MHD-instabilities of the whole plasma and for micro-fluctuations connected with the plasmoid were observed. The results of ITCS calculations agreed very well with measurement results. This fact finally proves both the full functionality of the ITCS calculations and the appropriateness of the physical models realized in the codes.

4. The second series of research experiments was carried out with enhanced parameters: Electron temperature about 100 eV, neutral beam power up to almost 1 MW and with pulse duration of about 4 milliseconds. Several important findings could be gained:

a. For the first time, the effect of ambipolar plugging was demonstrated in a mirror machine of gas dynamic trap type. It can be used for substantially improving their plasma confinement efficiency.
b. With increasing neutral beam power the appearance of electro-magnetic oscillations (micro-fluctuations) was observed if the maximal fast ion density exceeded the value of $2.5\times10^{13}$ $cm^{-3}$.
c. Unexpectedly, the micro-fluctuations did not result in a degradation of the fast ion confinement quality. Even, the measured fast ion densities were in good agreement with the results of ITCS computations reflecting the classical plasma physics. This "co-existence" of micro-fluctuations and validity of classical fast ion confinement remained up to the last experiment with a NBI power of ~0.9 MW in which the record value of fast ion density of $4.2\times10^{13}$ $cm^{-3}$ was achieved.

5. With regard to the GDT based neutron source project, the observation of the micro-fluctuations requires to draw the following conclusions:
   a. The nature of the oscillations must be clearly identified.
   b. Their dependencies on $\beta$, on the fast ion plasmoid density $n_f$ and on the degree of anisotropy $A$ of the fast ion velocity distribution must be investigated.
   c. Technical possibilities for efficient damping and limiting the oscillations must be searched for.
   d. These objectives need new theoretical and experimental research at the GDT-SHIP facility.

6. A first test series of experiments with deuterium injection was carried out. Unfortunately, the neutron measurement technique available was not yet calibrated. In spite of this, neutron transport test calculations with the Monte Carlo code MCNP [8] were carried out. In this way, appropriate modeling the geometry and the neutron source were tested. The results obtained enlighten the dependencies of the neutron field around the SHIP container on space and energy. From this, advices for favorable detector positions and regarding the calibration of the detectors can be drawn. Moreover, a calibration seems to be possible with help of well measured experiments with deuterium injection on the one hand and with ITCS and MCNP calculations on the other hand.

7. In recent GDT experiments in which high $\beta$-values appeared in the regions of fast ion turning points a gathering of the ions around the axis occurred during a time less than the collision time. At present, the ITCS codes do not reflect this effect within their framework of classical plasma physics based on Coulomb collisions and charge-exchange reactions. As in high-$\beta$ experiments planned for SHIP this phenomenon must also be expected, theoretical and numerical studies were carried out within the project in two directions:
   a. The analyses of simplified two-dimensional models (considering plasma behavior only in a transversal plane) which already had been started in the Budker Institute, were continued aiming at full clarification of the mechanism of such a self-organizing effect. The study showed that the plasma system with fast ions compacted around the axis is in a state in which the total energy is really in a minimum. Therefore, the transition from the initial into the compacted state takes place via degrees of

freedom provided it is permitted by the Liouville theorem. However, the result obtained cannot be transferred to the true three-dimensional case.

b. A first step of an analysis in three dimensions was done with the aim to identify the reason and the mechanism of the observed self-organizing effect. The study revealed that a certain class of ion trajectories having resonances between their longitudinal bounce oscillations and azimuthal rotations could make possible that ions can move a sufficiently long distance in radial direction. The results of numerical simulations show that such a stochastic ion transport can occur provided the magnetic field is locally perturbed by more than 3 %. However, this result also shows that the field perturbation caused by the asymmetry of the actual neutral beam injection system of the GDT is not strong enough for that. Consequently, the true cause and mechanism of the self-organizing effect observed in GDT experiments are still not clear. Further research is necessary for clarification.

8. Regarding the future development of the ITCS, the project showed that the code system should be extended beyond the framework of classical plasma physics. This seems to be necessary because one can expect that with further increase of plasma parameters up to values which are close to those of a real neutron source, the appearance of non-classical effects becomes more likely.

## 7. References


[1] Mirnov V.V. and Ryutov D.D. 1979 *Sov. Tech. Phys. Lett.* **5** 279

[2] Ivanov A.A. and Ryutov D.D. 1990 *Nucl. Sci. Eng.* **106** 235

[3] Post R.F. 1999 *Trans. Fusion Technol.* **35** 40

[4] Anikeev A.V., Bagryansky P.A., Ivanov A.A., Karpushov A.N., Korepanov S.A., Maximov V.V., Murakhtin S.V., Smirnov A.Yu., Noack K. and Otto G. 2000 *Nucl. Fusion* **40** 753

[5] Bagryansky P.A. et al. 2004 *Fusion Eng. Des.* **70** 11

[6] Ivanov A.A., Karpushov A.N. and Lotov K.V. 1999 *Trans. Fusion Technol.* **35** 107

[7] Anikeev A.V., Karpushov A.N., Collatz S., Noack K., Otto G. and Strogalova S.L. 2001 *Trans. Fusion Technol.* **39** 183-186

[8] X-5 Monte Carlo Team 2005 *MCNP – A General Monte Carlo N-Particle Transport Code, Version 5*

[9] Noack K., Otto G. and Collatz S. 1999 *Trans. Fusion Technol.* **35** 218

[10] Noack K. 2000 *International Conference "Monte Carlo´2000", October 23-26, 2000, Lisbon, Portugal, Proceedings 1063*

[11] Trubnikov B.A. 1963 *Voprosy teorij plazmi, Vol. 1, Atomizdat, Moscow*

[12] Collatz S. and Noack K. 1999 *Trans. Fusion Technol.* **35** 375

[13] Bagryansky P.A., Bender E.D., Ivanov A.A., Karpushov A.M., Murakhtin S.V., Noack K., Krahl S. and Collatz S. 1999 *J. Nucl. Mater.* **265** 124

[14] Maximov V.V., Anikeev A.V., Bagryansky P.A., Ivanov A.A., Lizunov A.A., Murakhtin S.V., Noack K. and Prikhodko V.V. 2004 *Nucl. Fusion* **44** 542

[15] Tsidulko Yu.A. 2004 *Phys. Plasmas* **11** 4420

[16] Lichtenberg A.J. and Lieberman M.A. 1983 *Regular and Stochastic Motion*, *Springer-Verlag, New York*

[17] Bagryansky P.A., Khilchenko A.D., Lizunov A.A. et al. 2005 *Trans. Fusion Sci. Technol.* **47** 327
[18] Bagryansky P.A., Den Hartog D.J., Fiksel, G. et al. 2003 *Rev. Sci. Instr.* **74** 1592
[19] Casper T.A. and Smith G.R. 1982 *Phys. Rev. Letters* **48** 1015
[20] Ishimura M. et al. 1993 *Phys. Rev. Letters* **70** 2734

## Acknowledgements

Both project partners are very grateful to Alexander von Humboldt Foundation for the financial support of the joint research project.

The project teams would like to thank those members of the GDT team, who were not explicitly included in the project, for their great deal of work with realizing the experiments for the project. Moreover, special thanks are expressed to Dr. P. A. Bagryansky, the leader of the GDT laboratory, for obligingly integrating the project work into the research plan of the GDT-SHIP facility.

The leader of the FZD project team, Dr. K. Noack, would like to thank all members of the GDT laboratory of BINP for fruitful collaboration for the idea of a GDT based neutron source over sixteen years which ends with this project.